Master Thesis

Optimization of pultrusion process parameters for flax fibre – reinforced thermoplastic composite tape production

Lorenzo Impelluso

TU Delft

Optimization of pultrusion process parameters for flax fibre – reinforced thermoplastic composite tape production

by

Lorenzo Impelluso

To obtain the degree of MSc in Materials Science and Engineering at the Delft University of Technology to be presented publicly in March, 2025

Supervisors:	Kunal Masania
	Georgy Filonenko
Place:	3me Faculty and AE Faculty, Delft
Project Duration:	March 2024 – March 2025
Student Number:	5599830

Table of Contents

List of Figures

List of Tables

Abstract

Thermoplastic matrices reinforced with natural fibres offer a promising solution toward the development of sustainable composite materials, which provide the potential for recyclability while lowering environmental impact. This research is particularly relevant to the growing sustainability concerns about WTBs (Wind Turbine Blades), predominantly manufactured from thermoset composites that are very difficult to recycle. These present huge EoL challenges due to the inability to efficiently process decommissioned WTBs, often leading to landfilling or energy-intensive recycling methods. In such a context, this work addresses the development of flax fibre-reinforced thermoplastic composite tapes via a lab-scale vertical pultrusion process. The focus will be to optimize melt pool temperature, pulling speed, and die geometry for high-quality, recyclable composites that are suitable for wind energy applications.

A custom machine was designed and produced to allow the combination of flax fibre twisted yarns and melted thermoplastic to make composite tapes by pultrusion. The influences of some key variables, for instance, consolidating die length, pulling speed, and processing temperature, on surface texture, void content, and fibre impregnation were studied. The results indicated that using a shorter consolidating die along with higher pulling speeds and high pultrusion temperatures, caused increased surface roughness. However, with an increase in the yarn count to reduce the gap between the fibres, the surface texture for the samples treated at 190°C (highest temperature tested) was significantly reduced.

Ultrasonic welding was also done, followed by lap shear tests to evaluate the weldability and mechanical strength of the tapes produced with the vertical pultrusion setup compared to benchmark samples. It was noted that the tapes processed at 190°C showed better mechanical properties compared to tapes processed at 170°C, which could be related to better fibre impregnation and higher crystallinity of tapes. Overall, the testing of welded samples showed that the mechanical properties of pultruded tapes were significantly superior compared to benchmark samples, as a result of stronger fibre-matrix bonding and considerably higher surface quality.

Future work should focus on refining die designs to further explore the effect of long tapered die sections, performing detailed crystallinity analyses, and employing advanced void measurement techniques.

1. Introduction

1.1 Motivation of the Thesis Project

Increasing concerns over global warming, environmental pollution, and the challenge of providing a reliable energy supply have made governments move away from fossil fuels in favour of renewable energy resources. Among all the sources, wind energy has appeared to be one of the most attractive; it has gained momentum over recent years and is supposed to play an increasingly important role in power generation during the coming decades. In fact, it is believed that by 2050, wind energy will contribute to 25 % of the production of Europe's electricity through an increase of its production by 82 % over its current production[1].

With this increasing demand for renewable energy, more and more blades used in turbines are being manufactured; usually these blades are fabricated from GFRP (Glass Fibre Reinforced Polymer). However, this has meant increased EoL (End of Life) waste generated, most of which because of the non-recyclable nature of the material goes into landfills[2,3].

The quest for sustainable solutions for WTBs (Wind Turbine Blades) at their EoL is, therefore, of growing importance. Current approaches to recycling, mainly mechanical and chemical methods, face huge challenges, such as energy-intensive processes and considerable degradation of material properties post-recycling. Notably, it is a quite energy-consuming process in case of glass fibres recycling: up to 93000 MJ/ton [4], whereas the manufacturing of new fibres consumes between 13000 and 30000 MJ/ton [3,4]. An alternative path lies in leveraging natural fibres like flax, which boast lower energy requirements for production (6000 MJ/ton), making them worth recycling [5]. Unlike synthetic fibres, natural fibres already fix carbon during growth at up to 1.39 kg of CO2 per kilogramme of fibre and thus partly equilibrate the quantity of CO2 emitted by their fabrication [6].

Interest in natural fibres has been increasing recently as it presents properties which make it a promising replacement for synthetic fibres in ecological reasons. Especially Flax Fibre is showing encouraging results on specific strength and stiffness [7]. If NF is combined with thermoplastic (TP) polymers, a composite material can be formed which at the end of life could be reshaped by taking advantage of thermoplastic's inherent properties. In fact, unlike thermoset resins, which are used predominantly in composite production, thermoplastics are not crosslinked and can be reheated and reshaped multiple times with minimal degradation, making them considerably easier to reuse and/or recycle [4].

LAFP technology is one of the methods that can be used to fabricate fibre-reinforced thermoplastic composite parts for large applications such as wind turbine blades with minimal waste and near net shape manufacturing compared to other techniques [8]. AFP employs continuous fibre composite tapes with constant cross-section, which are overlayed to produce parts. In order to produce these tapes, several methods have been developed, but the vast majority of them were researched for synthetic fibre. One of the most effective techniques to produce continuous fibre composite with constant cross-section like composite tape is pultrusion.

Compared to other composite manufacturing processes, pultrusion has several advantages such as high production rate of up to 5 meters per minute, and a more efficient and inexpensive process [9,10]. In addition, pultrusion can produce profiles that are practically unlimited in length which is ideal for continuous tapes. Even though pultrusion is being used extensively for synthetic material, the potential of combining thermoplastics with natural fibres remains fairly unexplored. Among all natural fibres, flax presents equivalent specific mechanical properties with glass fibres, a tensile strength of 38-52 MPa and 550-1030 GPa stiffness, which places it as an eligible

reinforcement material for composites [11]. The development of flax fibre-reinforced thermoplastic pultruded composites could give an environmentally friendly solution for producing continuous reinforced profiles and support the transition away from synthetic, non-recyclable material [10,12].

1.2 Research Objective

In this work, an attempt is made towards developing a small-scale vertical pultrusion setup that could manufacture tapes based on flax fibres and polypropylene matrix without applying any form of pressure from the outside. The design of the setup facilitates rapid testing of various fibre and matrix combinations while allowing for adjustments to manufacturing parameters. In order to evaluate the impact of these parameters, some key quality indicators are tracked (e.g. surface texture) which allow to assess the effectiveness of the setup. The insights and findings from this study will be able to provide the basis for further research and development of an accurate pultrusion setup capable of producing composite tapes apposite for LAFP.

To answer the research objective, four sub-questions have been elaborated. Each one of these has a very important role for leading the project toward its objective. These questions are:

1. What is the influence of die geometry on the impregnation and consolidation of the pultruded profile?
2. How does the temperature gradient and cooling rate along the die influence the tape's surface texture?
3. To which extent is the pulling speed altering the tape quality?
4. To which extent is it possible to optimize impregnation quality and void content without having to apply external pressure in a pultrusion process?

Answering those questions will be crucial for the development of a manufacturing process able to produce high quality natural fibre-reinforced composite tapes.

1.3 Structure of the Report

Chapter 1: An overview of the master thesis project, its motive, and the key research questions that need to be resolved.

Chapter 2: The chapter starts with an in-depth discussion on the mechanical and chemical properties of natural fibres, namely flax fibre and flax fibre composites. Then, thermoplastic composite tapes and the Tape Laying technology are explained and an overview of tape impregnation methodologies available is presented. Further, a detailed explanation of processing methods particularly experimented on flax fibre reinforced thermoplastics is presented.

Chapter 3: This chapter comprises a detailed explanation of the materials used, along with an explanation of the test setup and operation. Furthermore, the different characterization techniques employed to study the composite tapes are introduced. Both testing phases are also described: 'Testing Phase 1,' where all the preliminary tests and initial findings are, and 'Testing Phase 2,' which was established in an attempt to further investigate some details based on phase one observations.

Chapter 4: The results are presented and discussed in great detail in order to draw valuable conclusions and define subsequent developments. This chapter is again divided into 'Testing Phase 1' and 'Testing Phase 2,' with the second phase following on from the results and discussions of the initial phase.

Chapter 5: This chapter contains a summary of report findings and conclusions.

Chapter 6: New ideas and research proposals for further work on this topic are proposed, which attempt to fill knowledge gaps identified by this research.

2. Literature Review

2.1 Natural Fibers in Composite Materials

2.1.1 Introduction

In the context of increasing global environmental challenges, there has been a concerted effort towards sustainable development, marked by encouraging green activities and materials. Sustainable development aims at balancing the interests of the present and future generations. This has led to the creation of eco-materials to reduce the impact of human activities on the environment. Composites, known for their mechanical advantages and light weight, are being redesigned to be more eco-friendly, particularly in industries like automotive and aerospace[13]. As can be observed from Figure 1 below, several industries are greatly investing in composite materials and making them more and more a part of their products.

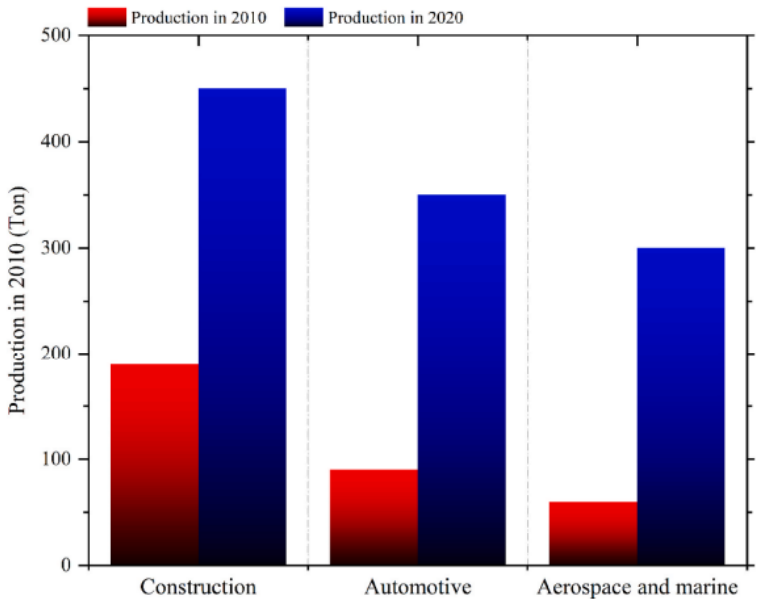

Figure 1: Comparison of natural fibre's production for different sectors [14]

Bio composites reinforced with natural fibre are coming forth as interest towards them is gradually increasing owing to their mechanical properties, low density and biodegradability. The demand for eco-friendly products is a global trend influenced by an overarching intention of lowering the carbon footprint and ensuring sustainability across industries. The journey towards the migration of composites to greener substitutes s aligns with efforts to minimize reliance on fossil resources and mitigate climate change. Furthermore, the use of bio-composites is cost-effective and available from renewable sources, enhancing their utility in many industries [13] . In fact, natural fibres may be sourced from plants (e.g., flax, hemp, jute, cotton), animals (e.g., wool, silk), and minerals (e.g., asbestos), all being renewable resources [15]. However, for the scope of this study, focus will be placed on plant based natural fibres.

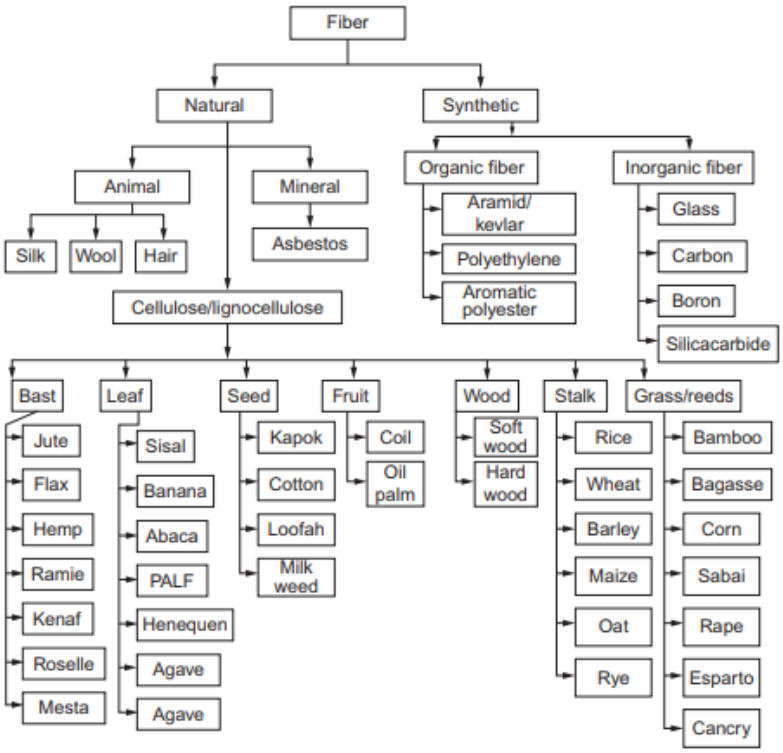

Figure 2: Natural fibres classifications[15]

2.1.1.1 Chemical Composition of Plant-based Natural Fibres

Plant fibres, made predominantly from cellulose and lignocellulose in nature, can be derived from a variety of plants, each possessing a unique composition of cellulose, hemicellulose, lignin, pectin, and waxes. Each of these imparts certain characteristics to the fibres depending on the plant source. [14]

Structurally, plant fibres are made up of two different walls: the primary and secondary walls. The primary wall is flexible and is made up of hemicellulose, pectin, proteins, and disordered cellulose microfibrils, and it forms a framework that gives support to cell growth. [13,16]

The secondary wall is thicker and rigid and is important in imparting mechanical strength to the fibre. As illustrated in Figure 3, the secondary wall has three layers: the outer layer (S1) 100–200 nm, the middle layer (S2) 0.5–8 nm, and the inner layer (S3) 70–100 nm. The lumen, an empty channel, is contained within the secondary wall for the transport of nutrients during plant growth. [13,14,16]

Structurally, the secondary wall contains more cellulose than the primary wall and also has lignin, which acts as a matrix, coating the tightly packed cellulose microfibrils arranged in a helical pattern. The cellulose chains are organized in microfibrils of size 2–20 nm and are bonded by amorphous regions, providing the fibre's overall stiffness and strength. [13,16]

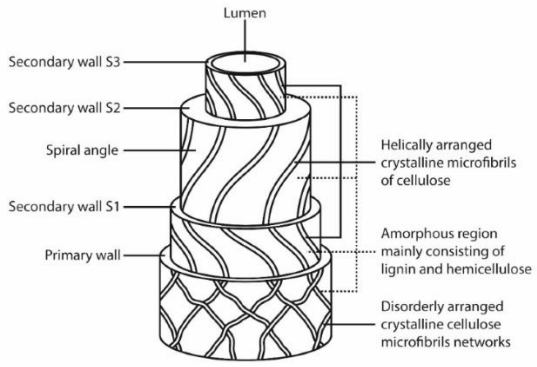

Figure 3: Structure of Natural Fibre [17]

2.1.1.2 Mechanical Properties

The mechanical properties of natural fibres are based on a number of key parameters. These are the fibre structure, chemical content, microfibrillar angle, and the presence of cell dimension imperfections. The presence of spiral-oriented microfibrils yields more flexible fibres, while microfibrils in alignment with the direction of the fibre yield more rigid fibres. Natural fibres also show wide variation in diameter along the axis of single filaments, contributing to their mechanical performance [16].

Chemical composition of natural fibres plays a central role in deciding mechanical properties. Microfibrillar angle—or spiral angle—also significantly influences fibre strength, with smaller angles indicating superior mechanical performance. For instance, coir fibres, with a relatively high microfibrillar angle of 41–45°, exhibit lower tensile strength compared to those of sisal (20°), PALF (14°), and flax (10°). Fibers such as jute, ramie, and hemp with microfibrillar angles of 5–10° are usually possess even higher tensile strengths [16].

Cellulose content is another important factor, as the fibres with greater cellulose content have greater tensile strength and Young's modulus due to the crystalline structure of cellulose [14]. The content of lignin also decides the structural properties and morphology of the fibres. Waxy material content is responsible for the wettability and adhesion of fibres, controlling the hydrophobicity of natural fibres, making bonding with matrices in composite materials more or less difficult [16].

On specific mechanical properties level, natural fibres are very similar to glass fibres [7]. As noted in Table 1 below, the specific strength of some natural fibres is at the same level as that of E-glass, showing their potential. Above all, flax fibre is characterized by its excellent specific mechanical properties, which, combined with its environmental advantages and weight-saving capabilities, make it an attractive alternative to glass fibre in some composite manufacturing applications.

Property	E-glass	Carbon (T300-T700)	Flax	Hemp	Bamboo	Jute
Density [g/cm^3]	2.55	1.8	1.45	1.48	1.4	1.46
Tensile strength [MPa]	2000–2400	3530–4900	800–1500	550–900	750–950	400–800
Stiffness [GPa]	70–74	230	55–75	40–65	30–50	10–30
Specific strength [MPa cm^3/g]	780–940	1900–2700	550–1030	370–600	535–680	275–550
Specific stiffness [GPa cm^3/g]	27–29	128	38–52	27–44	21–36	7–21
ε [%]	3	1.5–2.1	1.5–2	1.6	1.9	1.8

Table 1: Comparing properties of Synthetic Fibres (Carbon and E-Glass) to Natural FIbres[7]

2.1.2 Flax Fibers

2.1.2.1 Structure and Composition

Flax or Linum Usitatissimum is an annual crop cultivated for its stem and seeds, which are exploited primarily for fibre production [18]. Flax typically grows to 0.6-1.2 m in height, with a 1-3

mm stem diameter. It is a crop of moderate climates, particularly in regions like the Mediterranean region, Europe, Egypt, and the Indian subcontinent [19–21].

Flax fibres are extracted from the plant stem and exhibit a complicated hierarchical structure. On the macroscopic level, the stem consists of layers like the bark, phloem, xylem, and a central void, while on the mesoscopic level, flax fibre bundles consist of 10 to 40 single fibres held together primarily by pectin. The complicated microstructure of the fibre is characterized by its hierarchical organization on various length scales and the varying proportions of a range of components [19–21].

On the cellular level, each elementary fibre contains concentric cell walls, and the secondary cell wall contributes the most to the fibre's strength. The S2 layer, the thickest layer of the secondary wall, is made of crystalline cellulose microfibrils and amorphous hemicellulose, oriented at a 10° angle from the fibre axis, and is accountable for the fibre's high tensile strength. On the nanoscale level, these cellulose chains have crystalline domains dispersed in an amorphous matrix that consists mainly of pectin and hemicelluloses. This structure makes flax fibres strong in addition to being versatile in their use [19–21]. Several studies have been conducted to determine the composition of flax and all of them reach the same findings as outlined in Table 2, whereby cellulose (65-75 wt%) and hemicellulose (15-20 wt%) are the two major constituents [22].

Cellulose (wt%)	Hemicellulose (wt%)	Pectin (wt%)	Lignin (wt%)	Wax (wt%)	Moisture content (wt%)
71–75	18.6–20.6	2.2	2.2	1.7	10
62–72	18.6–20.7	2.3	2–5	1.5–1.7	8–12
64.1	16.7	1.8	2	1.5	10
73.8	13.7	–	2.9	–	7.9
71–78	18.6–20.6	2.3	2.2	1.7	7

Table 2: Composition of Flax Fibre as described by different sources [22]

2.1.2.2 Mechanical Properties

The tensile mechanical behaviour in flax fibres is determined to a very large extent by their length, with the shorter fibres possessing high tensile strengths. As evidenced from the graphs in Figure 4, simple fibres at a clamping length of less than 3 mm have their tensile strength at about 1522 ± 400 MPa. Technical fibres, which are 100 mm in length, have tensile strengths between 500 and 850 MPa depending on their length. Reducing the fibre strength reduces the fibre structure impurity by decreasing critical flaws, which in turn leads to higher tensile strength [23].

As the fibre length increases, the failure mechanism also changes. Short fibres will fail in tension by stress in their hard cellulose walls, but longer fibres will fail in shear within the pectin-rich interphase. Compression tests, such as the elastic loop test, show that the flax fibres can register compression strengths of approximately 1200 ± 370 MPa [23].

Experiments by H.L. Bos et al. reveal no noticeable difference in the stress-strain curve between different types of flax fibres, e.g., hand-isolated fibres (kink-band-free, see Figure 5) and normal fibres, which means that the Young's modulus is identical for both types. Compressive failure appears to occur when the kinking phenomenon spreads over the entire diameter of the fibre [23].

Aside from the promising mechanical properties of flax fibre, it is important to mention that, compared to its synthetic counterparts (carbon or glass fibre) flax fibres are highly hydrophilic due to their high cellulose content, and water absorption would seriously impair their mechanical properties. Static and dynamic moduli decrease with increasing relative humidity, which negatively affects their overall strength and behaviour [18].

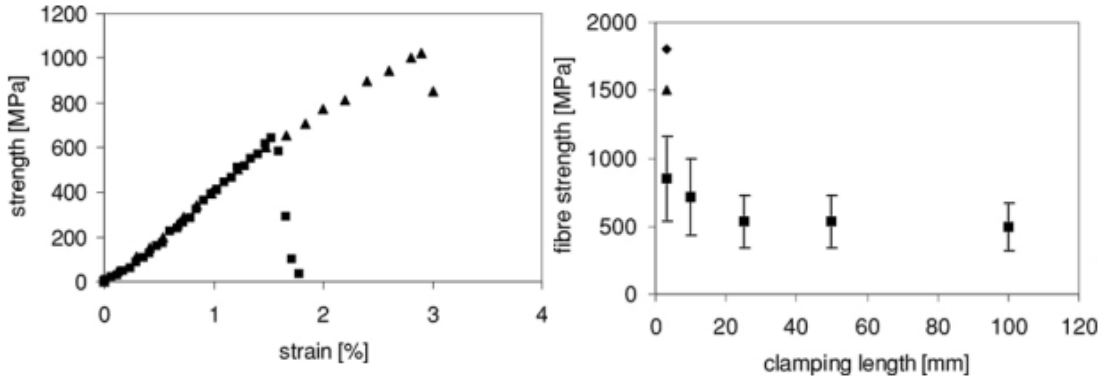

Figure 4: Stress-strain curve for technical fibre (Left); Tensile strength vs clamping length for technical fibre (Right) [23]

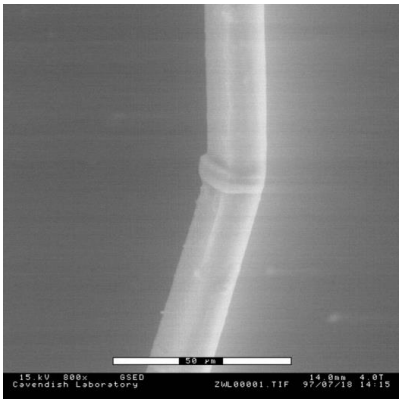

Figure 5: ESEM image of a kink band [23]

2.1.3 Flax Fibers on Composites

2.1.3.1 Polymer Matrix

The polymer matrix in natural fibre/polymer composites plays several significant functions [18].

- **Load Distribution**: The matrix retains the fibres, fixing their position and transferring loads between the fibres by adhesion and/or friction.
- **Provide Rigidity and Shape**: It imparts rigidity and shape to the structural component.
- **Protection**: The matrix protects fibres from chemical corrosion and other environmental factors.
- **Influence Performance**: It affects performance behaviours like impact resistance and ductility.

The polymer matrices are classified into two broad categories: Thermoplastics and Thermosets. Thermoplastic polymeric matrices (TPPM) show reversible curing, softening on heating beyond their glass transition temperature (Tg) or melting point (below their decomposition temperature). When cooled, they become hard again, and the process can be repeated. With linear or branched molecular structures, TPPM are solvent-soluble, tough, chemical and water-resistant. Thermosetting polymeric matrices (TSPM) cure irreversibly to produce rigid, cross-linked networks. TSPM, unlike TPPM, are not re-mouldable or re-meltable upon heating, instead they degrade upon continuous heating. However, TSPM are stiff, tough, durable (because of their large molecular size), electric and heat insulators, and chemically resistant [24].

Thermoplastic Composites (TPCs) have recently gained popularity across various industries thanks to their time and cost-effective manufacturing. TPCs do not undergo a cross-linking reaction when they consolidate compared to thermosets, and hence no post-curing cycles are needed. Because of this, they solidify easily under pressure and temperature and cut-down on the long curing periods that are intrinsic to thermosets. The said characteristic not only saves time and cost but allows more automatic assembly lines to be created as well, rendering various advantages for TPCs [25].

In addition, TPCs possess the advantage of heat reforming after use, which enhances recyclability and remanufacturing. As environmental and economic consciousness rises, recyclability of thermoplastic composites (TPC) is crucial. The ability of TPCs to be reprocessed multiple times also enhances repair convenience and polymer welding, hence reducing time consumption for maintenance tasks [26].

As can be seen from Figure 6 below, there are different thermoplastic polymeric matrices that are available and suitable for a variety of different uses. For instance, in the aerospace industry, high performance thermoplastic matrix materials such as PEI, PEEK, PEKK, LM PAEK, PPS, and ABS thermoplastics are commonly used and are reinforced with glass fibre (GF) or carbon fibre (CF) for the most part [26]. The high tensile modulus and tensile strength of these high-performance thermoplastics relative to other thermoplastics (as shown in Table 3), along with their high abrasion and high temperature resistance, are what make them 'high-performance'.

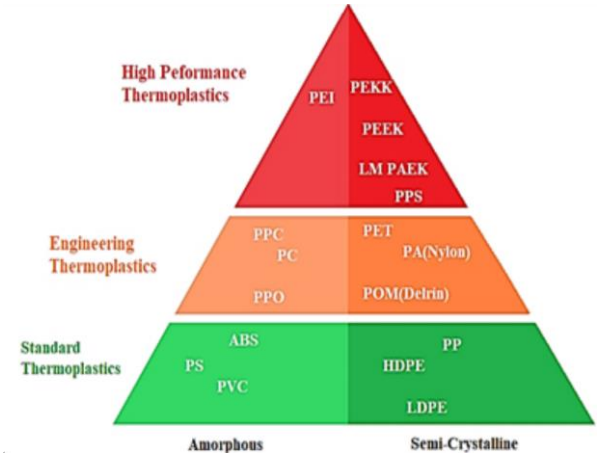

Figure 6: Thermoplastic matrices divided in categories based on their properties [26]

Materials	Tensile Modulus, GPa	Tensile Strength, MPa	Melt Flow, g/10 min	Melting Point, ˚C	Density, g cm^{-3}
Polypropylene (PP)	1.5 – 1.75	28 – 39	0.47 - 350	135 - 165	0.89 – 0.91
Polyethylene (PE)	0.15	10 – 18	0.25 – 2.6	104 – 113	0.918 – 0.919
Poluyurethane (PU)	0.028 – 0.72	5 – 28	4 – 49	220 – 230	1.15 – 1.25
Polyamide (PA)	0.7 – 3.3	40 – 86	15 – 75	211 – 265	1.03 – 1.16
Poly phylene sulphide (PPS)	3.4 – 4.3	28 – 93	75	280 – 282	1.35 – 1.43
Polybutylene terephthalate (PBT)	1.75 – 2.5	40 – 55	10	230	1.24 – 1.31
Poly ether ketone ketone (PEKK)	4.4	110	30	360	1.31
Poly ether ether ketone (PEEK)	3.1 – 8.3	90 – 11	4 – 49.5	340 – 344	1.3 – 1.44
Poly ether imide (PEI)	2.7 – 6.4	100 – 105	2.4 – 16.5	220	1.26 – 1.7
Polyether sulphone (PES)	2.4 – 8.62	83 – 126	1.36 – 1.58	220	1.36 – 1.58
Poly ether terephthalate (PET)	2.47 - 3	50 – 57	30 - 35	243 – 250	1.3 – 1.33
Polyoxymethylene (CoPOM)	2.7	63	11	166	1.41
Poly-L-lactic acid (PLLA)	3.5	69	6 - 7	180	1.24 – 1.29

Table 3: Collection of properties from different thermoplastics [27,28]

2.1.3.2 Manufacturing Methods

Depending on the matrix and the quality or purpose of the final product to be achieved, various manufacturing processes have been developed over time to meet different needs. Some of the most important processes are:

- **Hand Lamination**: One of the most basic and inexpensive methods of composite preparation, involving the manual application of the resin and reinforcing elements to an open mould [29].
- **Spray-Up**: Involves spraying resin with cut fibres into a mould, suitable for thermoset composites and can be manually or automatically done [29].
- **Pre-preg Lay-Up**: Involves laying down pre-impregnated fibre layers on a mould, often used manually but with automatic facilities available [29].
- **Resin Transfer Moulding (RTM)**: Standard method of injecting resin into a sealed mould with the reinforcement, applicable to most types of material and large-scale production [29].
- **Compression Moulding**: Applies pressure and heat in a sealed mould to cure/consolidate composite, suitable for both thermoplastics and thermosets with varying pressure profiles and uses [29].
- **Tape Laying**: One broad, unidirectionally reinforced tape is utilized in tape laying to lay up flat composite parts or simple contours with fibre direction control and allowing automated fibre placement [30].
- **Filament Winding**: Suitable for cylindrical shapes, which involves impregnation of roving or yarns with resin and winding on a rotating mandrel [29].
- **Pultrusion**: Efficient method for continuous cross-section elements, consists in drawing impregnated rovings through a die, curing or consolidating and sawing to length, well suited for high fibre volume fractions and end use in transport or building materials [29].

2.1.3.3 Mechanical Properties

In terms of mechanical properties of flax composites, considering longitudinal stiffness, unidirectional flax composites possess comparative mechanical properties to glass fibre composites. However, as the flax is lighter in weight, the specific stiffness of flax fibre composite materials (FFCM) is higher than that of glass fibre composites at times as is also clear from Figure 7(b) [11] . Besides, in Figure 7(c) it can be seen how flax also shows remarkable performance in plate bending applications, beating steel as well as aluminium in specific bending stiffness, and lagging only 15-25 % behind carbon fibre reinforced polymers (CFRP) when the fibre volume fraction is between 30-60 % [11].

Looking at strength, the relative comparison of flax fibre composites to other fibre composites is more complicated. Strength depends on the fibre architecture type (e.g., non-crimp fabric, weave, braid, mat), which influences flax fibre composites less predictably than stiffness. Literature shows that the specific strength of cross-ply (0/90) flax composites is approximately half that of glass fibre composites at a volume fraction of 40% [11] .

Flax fibers also offer better vibration damping properties, at least 2.5 times higher than carbon fiber composites. This is because of the complex microstructure of flax, which consists of weakly bonded elementary fibers and crystalline microfibrils in an amorphous matrix [11].

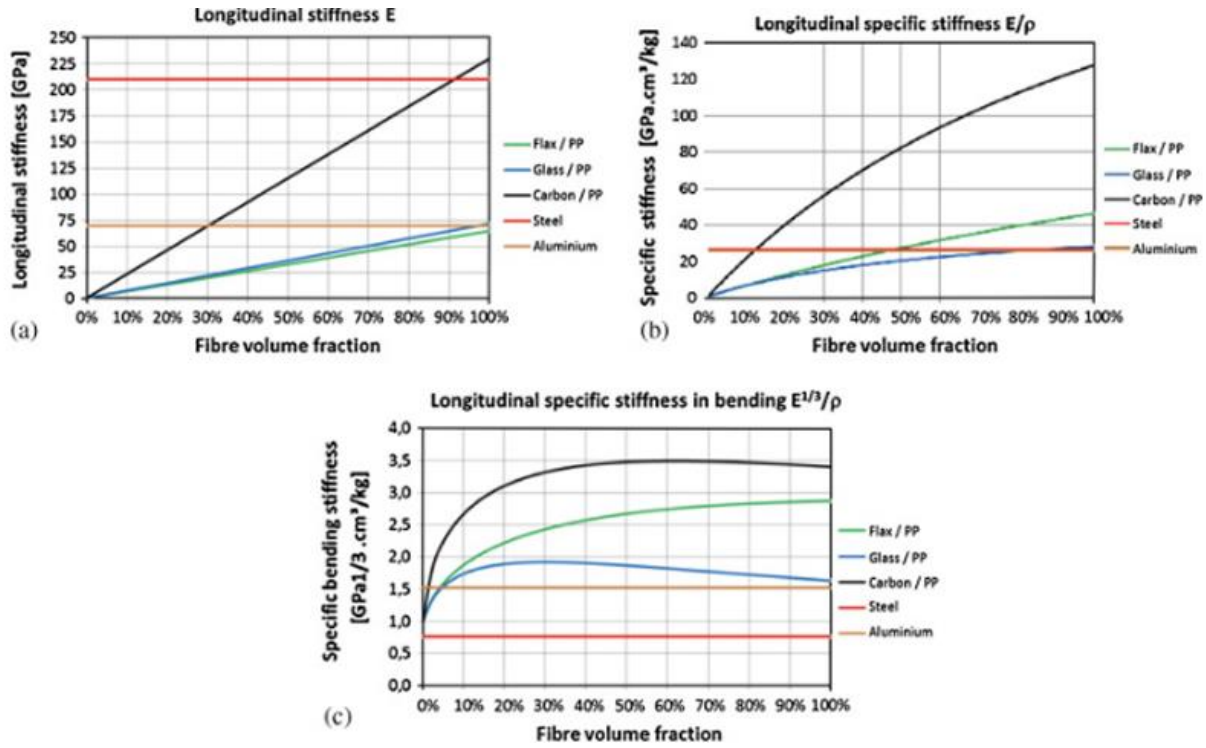

Figure 7: a) Longitudinal modulus, b) Specific longitudinal modulus in tension and c) Specific longitudinal modulus in bending for fibre UD composites of flax/PP, glass/PP, carbon/PP as well as for aluminium and steel in relation to their fibre volume fraction.[11]

2.2 Thermoplastic Composites in Tape Laying Manufacturing

2.2.1 Tape Laying

Tape laying, or fiber tape placement, was initially developed for the aerospace industry to produce optimized aircraft panels in a cost-effective way, compromising between cost and complexity. In recent years, its application has found its way across a number of industries due to its advantages related to manufacturing flexibility and control, and time saving in large scale applications. This technique uses wide, unidirectionally reinforced tapes to form simple contours or flat composite parts, offering precise control of fiber orientation and enabling automated fiber placement. It is particularly valuable for reinforcing localized regions of components with unidirectional strips [31].

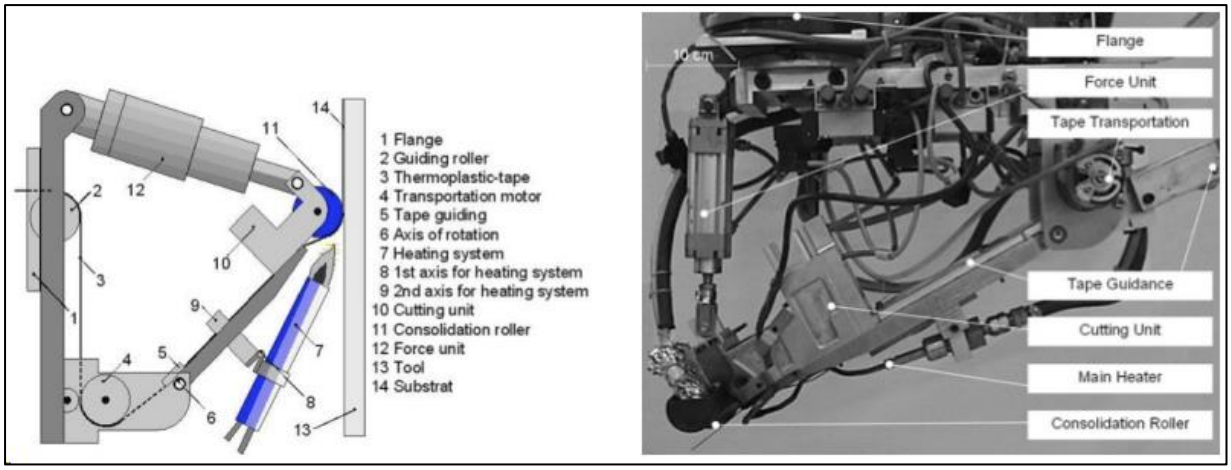

Figure 8: Tape Laying Setup [32]

The tape laying equipment used for thermoplastic composites is described in Figure 8 and it employs a multi-axial gantry system or a 6-axis robot to position and orient the tape placement head (TPH) on large structures. The TPH has a feeding unit for delivering the tape, a consolidation device for applying pressure, and a cutting device for trimming the tape after placement. During the process, the tape is brought above its melting point and consolidated onto the mold surface or the previously deposited layer. Various heat sources, including flame, ultrasonic, infrared (IR), induction, and laser, have been tried, with laser heating being most successful due to its high energy density, efficiency, and quick response time[32]. For the manufacturing process to be achievable, it is necessary for the composite tapes to be pre-impregnated with the thermoplastic matrix as it is currently not possible to lay dry tapes and inject or infuse them with thermoplastic. Correspondingly, different methods are devised for the pre-impregnation of fibers and the effective production of thermoplastic composite tapes.

2.2.2 Thermoplastic Composite Tape

Tape for tape laying is produced through sophisticated impregnation processes like powder, melt, belt, or slurry processes where the fiber is fully impregnated with matrix material [33,34]. Usually with fiber volume contents of 30 % to 70 %, tapes are reinforced by glass fibers (GF) or carbon fibers (CF), but there is a growing interest in the utilization of natural fibers (NF) [31]. The tape thicknesses range from 0.13 to 2.5 mm, with the option of custom thicknesses for specific applications, and widths of 1 to 150 mm, which are tailored during manufacturing [35]. Commonly employed matrix materials include polypropylene (PP) owing to its low cost and polyetheretherketone (PEEK) owing to its high performance. Thermoplastic composite tapes can be processed by a variety of techniques, which include tape placement, winding, and traditional compression molding, making them versatile and ideal for high-value applications like LATP [31]. As expected, the processing techniques employed has a considerable influence on the final quality of the component. However, the quality of the starting material is just as important, hence, several tape quality parameters have been identified to evaluate the starting material.

2.2.2.1 Tape Quality Indicators

Achieving a balance of key manufacturing parameters is essential to produce high-quality tapes, which play a vital role in the production of uniform, high-performance parts using Laser-Assisted Fiber Placement (LAFP).

Low void content and low surface roughness are the primary features of high-quality tapes. Low void content is crucial for rapid automated processing because higher void content tapes require longer consolidation (longer heating times and additional pressure) to reduce the voids [35] . It is worth mentioning that 2 % of void content is acceptable for pultruded profiles (based on the DIN EN 13706 standard) however this parameter does not hold for aerospace usage[36].

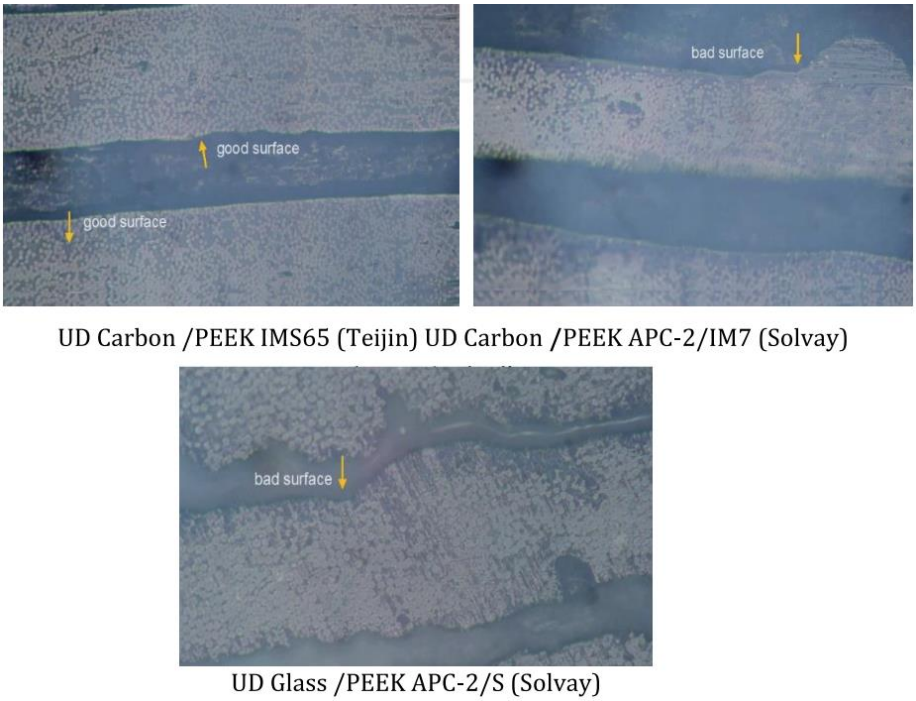

Figure 9: Microscopic images of raw material to show surface quality [35]

Similarly to void content, surface roughness is also a very important factor in the LATP/LAFP process. During layer stacking, complete intimate contact is achieved if the materials are smooth. When the surfaces are uneven, it can lead to inter-laminar void content formation, resulting from poor intimate contact [35]. These voids can act as crack initiation sites, as voids are stress concentrators, and reduce the mechanical performance of the end product, e.g., inter-laminar shear strength, compression and transverse tensile strength. Figure 9 shows examples of good (flat) and bad (rough) surface roughness and how that affects the uniformity of the end product.

Finally, usually a thin tape thickness is desirable as it offers more design freedom allowing the TPH to wind and bend the tape around intricate shapes. Thin tape thickness also enables good and even heat transfer, which is required for efficient layer adhesion and allows for acceleration of the production process [35].

2.2.2.2 Common Tape Manufacturing Methods

Production of tape involves various methods for impregnating polymer into fibers for the fabrication of composite tapes that are strong. The major methods are mentioned below.

Solution Impregnation: Due to the high melt viscosity of thermoplastic resins, the creation of thermoplastic composite prepregs through impregnating polymer fibers with a polymer solution arises, which eases wetting of fibers. The process involves the transfer of reinforcement through a bath of solvent/polymer solution, followed by a solvent evaporation unit where the solvent is removed using heat leaving behind the resin. While the aim is to remove solvent in its entirety,

there can be residual solvent in the impregnated fiber that can create voids in subsequent processing phases [37].

Melt Impregnation: During melt impregnation, fibers are unwound from a spool and heated to or above the polymer melt temperature. An extruder blends and melts the thermoplastic and the heated fibre tow is impregnated with molten resin in a die. Melt baths may include pins mounted to allow movement of fiber strands along a desired path and stretching them out to assist with impregnation [38].

Powder Impregnation: In powder impregnation, the fiber tow is first unwound from a spool and passes through a spreader for dispersion. The spread tow then enters an impregnation chamber where particles are attracted to the fiber by electrostatic forces or because of a binder on the fiber surface. The fiber is then passed through a heater where the powder is sintered onto the fiber surface. Finally, the flexible tape formed is wound onto a take-up drum [39].

Aqueous suspension impregnation: Aqueous suspension coating involves suspending polymer particles in water. The reinforcement material is passed through this suspension, where the matrix particles adhere to it. Then, the impregnated fibers are passed through a hot region to evaporate the liquid and sinter the matrix particles on the reinforcement [33].

These methods are prevalent and effective for synthetic fibers. It is challenging to achieve consistent high-quality tapes from natural fibers due to their structure and hydrophilic nature [16]. Different methods can be found in the literature, testing different production processes for natural fiber thermoplastic tapes. The following paragraphs introduce the methods explored in recent studies.

For instance, in solution impregnation with compression molding, as McGregor [31] describes, twisted flax yarns are impregnated with PLA in THF, then solvent is evaporated and finally pressure is applied to the tape to consolidate it, as shown by the diagram in Figure 10. The process yields a 10 mm wide tape made up of 35 parallel yarns. Maximum values were achieved at a 2 MPa pressure and a fiber tension of 15 N, producing a tape whose tensile modulus and strength were 196 MPa and 16 GPa, respectively.

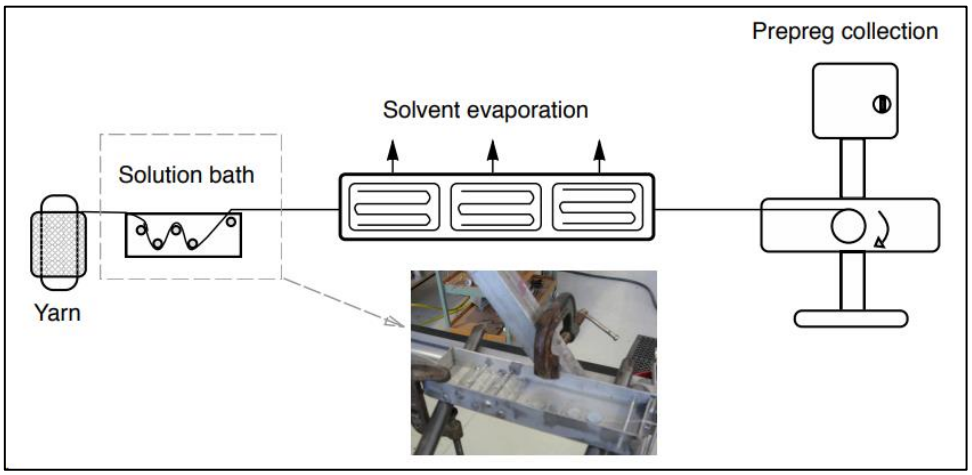

Figure 10: Solution Impregnation Diagram, involving a THF/PLA bath followed by an evaporation step to remove the solvent[31]

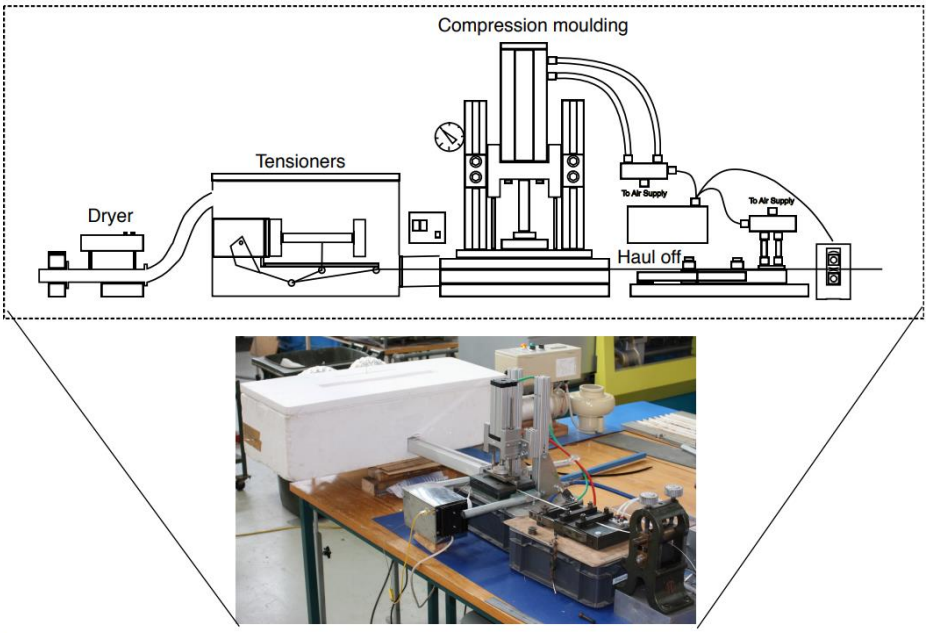

Figure 11: Continuous Compression setup used to impregnate and consolidate the tapes in the desired shape[31]

McGregor[40] also reported another production process whereby polyamide was employed in powder-water slurry for coating twisted flax yarns and is illustrated in Figure 12 below. The coating step was followed by a water evaporation and powder sintering step for melting the polymer onto the yarns, then heated rolls were used for tape consolidation. The process yielded 6mm wide tapes with 25 parallel yarns and the best properties were achieved at 80 mm/min haul off speed and 210-220˚C heating temperature for the water evaporation and powder sintering process. McGregor's best tape could achieve tensile strength 222 MPa and tensile modulus 23.1 GPa with a 11.5 µm surface roughness.

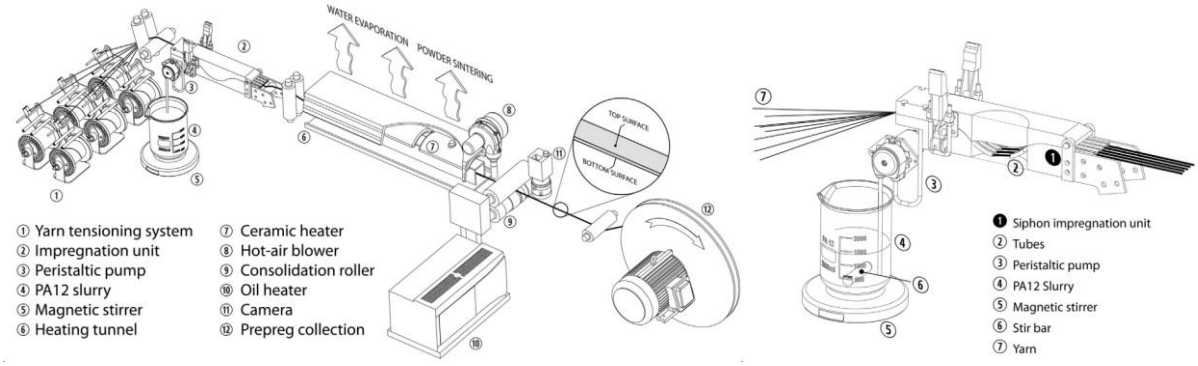

Figure 12: Diagram of Slurry Impregnation (aqueous) followed by an evaporation step and Consolidation Rollers[40]

Moving away from solvent and aqueous impregnation, Hartung et al [41] conducted two parallel studies for two different production processes. In the two studies, unlike McGregor's twisted flax fiber yarns, Hartung et al used combing flax fibers with a mean length 128 mm, which underwent two drafting processes so as to align the fibers parallel to the winding direction. The initial study was on Film-stacking-draft (FSD) process, as shown in Figure 13, in which flax fibers and polypropylene (PP) films are stacked, heated, and pressed in a double belt press where impregnation and consolidation take place. The second process was the commingled-sliver-draft (CSD) process, as shown in Figure 14, where flax and PP fibers are drafted together to align the

fibers in the direction of pulling, and then the same operation with the double belt press is used to melt the polymer and consolidate the tape through heat and pressure. Overall, Hartung et al concluded that CSD exhibited better mechanical properties than FSD because of its improved micro impregnation. This is likely related to FSD´s higher void percentage which could be attributed to air and moisture that was being trapped in the structure by the films. The tapes produced were 200mm wide and approx. 0.2 mm thick with 50 % fiber weight percentage. In order to evaluate the tensile properties of the CSD samples, two tape pieces were stacked and the maximum tensile strength and modulus recorded were 200 MPa and 19.0 GPa, respectively.

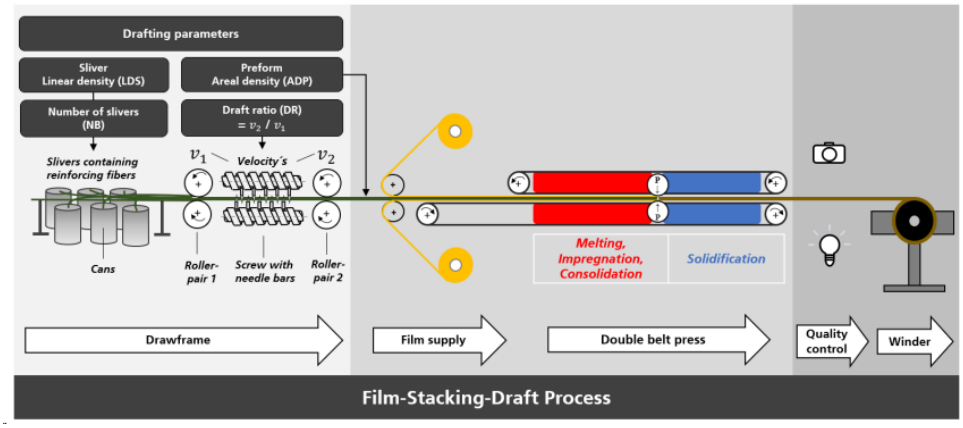

Figure 13: Film-Stacking Draft Process Diagram to produce composite tapes[41]

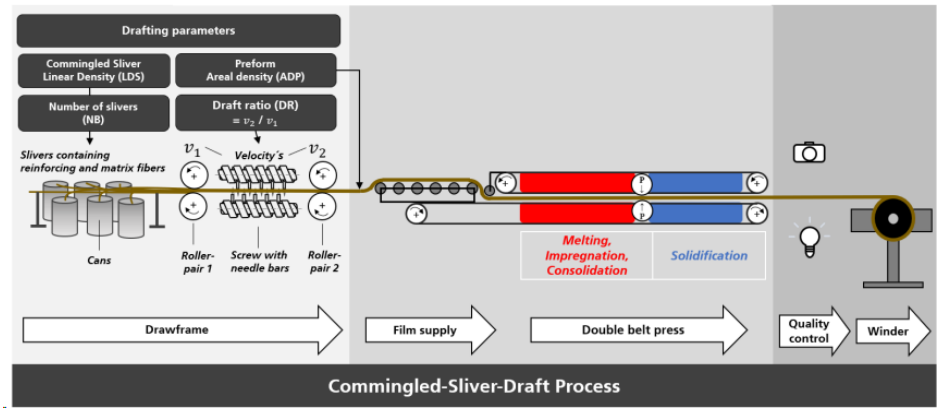

Figure 14: Commingled-Sliver-Draft Process Diagram to produce composite tapes[41]

Finally, Akonda et al [42], had a similar process to Hartung´s CSD process, however with consolidation rollers instead of belt press. Similarly to Hartung et al, this process starts with carding and drafting flax and PP fibers, then heat and pressure is applied using rollers to create a consolidated tape. The tapes produced were 0.6 mm thick, 18 mm wide and had a 50% fiber weight percentage. The mechanical tests were carried out on tapes that were stacked and consolidated together to make a 2mm thick laminate with around 2-3% voids and a flax volume fraction of 38.5%. The ultimate tensile strength and modulus were found to be 125 MPa and 22 GPa, respectively.

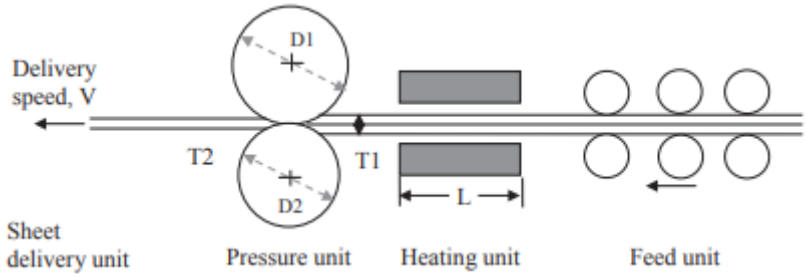

Figure 15: Commingled-Sliver-Draft Process with Consolidation Rollers to produce composite tapes[42]

Research on producing flax fibre composite tapes and impregnating these tapes with various thermoplastics is currently limited to the studies presented above. Nearly all processes described contain a minimum of two stages: impregnation and consolidation. With the use of slurry or solution impregnation, there is a further evaporation or drying stage. Moreover, in some cases twisted flax yarns are not employed, but rather a Flax/PP fiber commingling is performed, which also increases the manufacturing process complexity. However, there is a method that would simplify the production process by combining impregnation and consolidation into a single step only using heat, as opposed to the belt press or consolidation rollers, which also involve pressure. This is referred to as pultrusion, where a series of heated and cooled dies are used to impregnate and consolidate the tape in a single, continuous process. While this process has been highly successful with synthetic fibers, no research has been reported on its application to flax fibers in tape manufacturing.

In the following section, an overview of thermoplastic pultrusion as an impregnation process will be presented with particular focus on the primary parameters in pultrusion and potential areas for further research.

2.3 Pultrusion

In recent years, thermoplastic pultrusion has been an important area of study in the field of composite materials, but nonetheless much less represented compared to thermoset pultrusion. While thermoplastic composites have inherent advantages such as increased impact toughness, recyclability, lower production time, and environmental benefits, they have had little application within industrial markets.

Several methods for making reinforced thermoplastics by pultrusion have been developed over the years, all of which involve inserting both the polymer and the fibers into a hot die cavity and then pulling it out from the opposite end. The die cavity contains a tapered part that is converges along the direction of drawing followed by a straight part that forms the final cross-sectional profile of the product.

Others methods that are currently used, comprise for example powder or solution impregnation processes, whereby a layer of polymer is applied on the fibers before drawing them through a heated die. Another common method is the commingling of polymer fibers with dry reinforcement fibers, which are drawn through the die. As seen in Figure 17, the process melts the polymer onto the fibers, essentially impregnating them. Lastly, melt injection is a technique where an extruder is equipped to the die cavity with a heating element, and as polymer melts it is gradually supplied into the die cavity while the fibres are simultaneously pulled through it, ensuring proper impregnation (Figure 16).

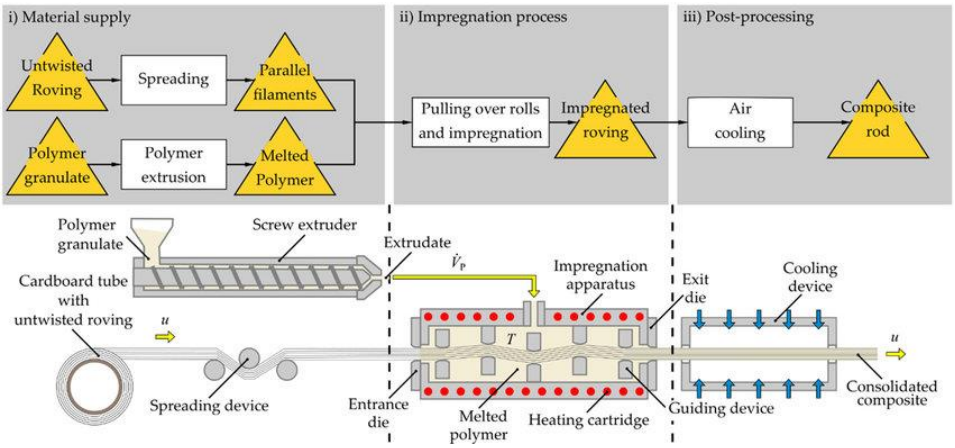

Figure 16: Schematic of a polymer injection pultrusion system[43]

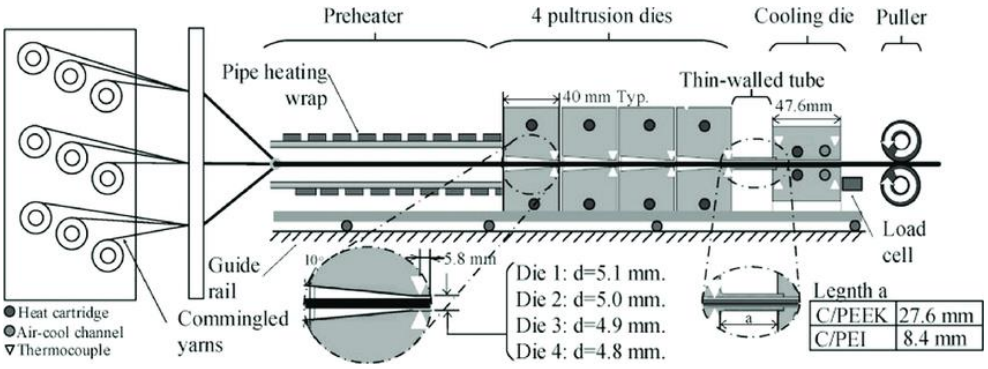

Figure 17: Schematic of the multi-die pultrusion system with commingled yarns[44]

2.3.1 Key Processing Parameters

With time, engineers have tested various parameters and constructed models in an effort to optimize the process of pultrusion for a range of fibre and matrix combinations. The parameters which were discovered to have an impact on the product quality were the rate of pulling, the heating and cooling die temperature, tension within the fibres and die geometry. Each of these parameters has an influence on the resulting product as elaborated below.

2.3.2 Pulling Speed

A rise in the pulling speed during the pultrusion process was seen to increase the pressure at the end of the tapered part of the die, thereby raising the degree of impregnation of fibres [45]. Pressure was mainly created as a result of the thermal expansion of the polymer inside the die and also as a result of the compaction of the polymer inside the die cavity due to continuous shearing of polymer into the die by the moving fibres. Figure 18 is a simulation of pressure gradient in an impregnation die of a pultrusion system. The simulation shows how shearing the polymer into a progressively tighter cavity causes a pressure build-up at the end of the die, which can be increased by increasing the pulling speed that will directly increase the shearing rate. On the other hand, high pulling speed can also lead to insufficient time for consolidation, thereby resulting in poor final quality [45].

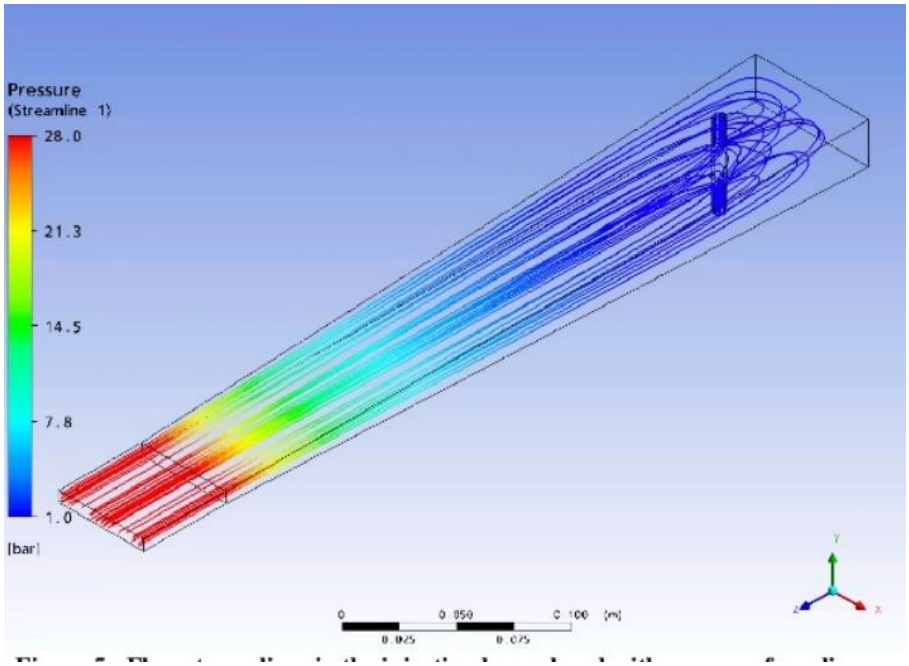

Figure 18: Simulation showing pressure gradient within heating die[46]

The pulling speed also has a direct effect on the pulling force, which plays a major role in the process of pultrusion. The force of pulling is influenced by various mechanisms, including friction (material friction on the die wall), viscous resistance (shear flow through the narrow gap between the pultruded mass and the die wall), and compaction resistance (compaction-induced resistance within the tapered zone of the heating die) [45,47]. As the pulling speed increases, friction, viscous and compaction resistance all rise, thus contributing to the higher pulling force needed [45].

Pulling speed was also observed to have an effect on the surface finish of the pultruded components [48–50] . The surface was observed to shift from a shiny to a rougher surface as a result of increased pulling speed beyond some threshold. This effect is caused by metal-polymer adhesion forces within the pultrusion die and it's known as the "sloughing" phenomenon. When the adhesion forces are greater than the pultrudate strength, pieces bond to the die surface and tear off from the pultrudate [48–50].

2.3.3 Heating Die Temperature

Another factor that affects the pultruded profile significantly is the heating die's temperature. The temperature of the heating die affects the viscosity of the polymer which decreases as the temperature rises. While low viscosity is necessary to be able to impregnate fibres in the right manner, too low viscosity will reduce pressure in the die cavity and therefore impregnation as well[36].

In addition, extremely low viscosity will not allow mechanical shearing of polymer along the polymer cavity into the tight straight die portion and will lead to polymer flowing in the reverse direction and collecting at the die entrance, causing poor fibre impregnation [36,50].

On the other hand, if the temperature of the heating die is not high enough, the polymer's viscosity is too high which, other than leading to inadequate fibre impregnation, greatly increases the pulling force required for pultrusion. With a pulling force that is too high, it can induce fibre breakage which would damage the pultruded part [45].

2.3.4 Cooling Die Temperature

Similar to the heating die temperature, the cooling die temperature is also critical to produce high quality pultruded profiles. The cooling die temperature mainly affects the surface texture of the pultrudate. It was observed that with increased and faster shrinking of the polymer in the die as a result of rapid cooling, the polymer de-bonded faster from the die wall and thus improved surface quality [49]. As explained in the pulling speed paragraph, the "sloughing" phenomenon reduces the surface quality, the impact of this phenomenon can be reduced to a large extent by rapid cooling of the polymer, which results in the shrinkage of the matrix [48,49] . Cooling dies can be air cooled or water cooled, however water cooling ensures a much more effective and even cooling, a picture of a water-cooled die is shown in Figure 19.

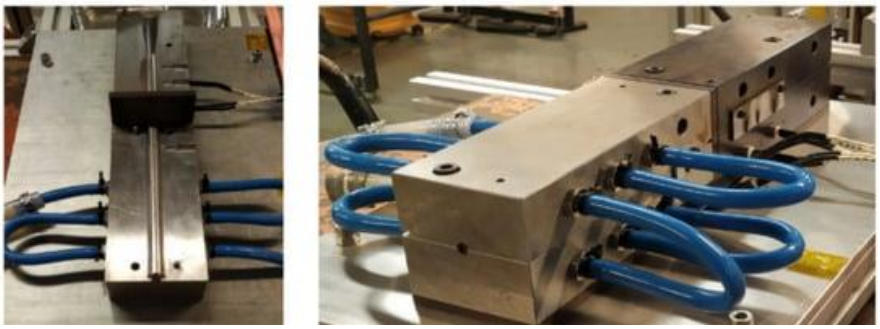

Figure 19: Water cooled die block[51]

Die temperature directly influences the temperature of the pultruded product as it exits the die. The best scenario is to cool the polymer to a temperature below the glass transition temperature (Tg), such that no loss of shape is incurred as a result of externally imposed forces or fibre relaxation (commonly referred to as "spring-back" action). However, for some polymers, the Tg is well below room temperature, and thus a more advanced cooling system would be necessary to achieve this. Although it is preferable to cool the polymer to its Tg, studies show that sufficient crystallization content can minimize distortion on die exit even if the polymer is not fully cooled to its Tg [10,45].

2.3.5 Spool tensioning

Research indicates the spool tension also affects the void content of the final product. In fact, too high tension in the spool leads to lower permeability of the bundles of carbon fibres due to them being too tightly packed, thus lowering the area of contact between the polymer and the fibres [49].

2.3.6 Die Geometry

Another essential aspect of fibre impregnation is the heated die block geometry. The die block is tapered, becoming smaller in the direction towards the die exit. Near the exit, the cross-section remains constant, which is similar to the form of the resulting composite. The die block taper angle affects the pressure and the backflow of the thermoplastic melt. A taper angle of 4˚ is a

suitable compromise between the pulling force required and pressure generated in the die provided that polymer viscosity is set properly [52]. The internal surfaces can be chromium-plated to reduce friction between the composite and internal die block surfaces, and to lower the pulling force [10,53]. In addition, some die blocks use special pins to force the thermoplastic melt into the fibres [10].

In conclusion, by optimizing key manufacturing parameters, pultrusion can be an extremely effective process for the production of continuous natural fibre tapes with a thin, uniform cross-section. The process could generate sufficient pressure in the die to impregnate the fibres and achieve a surface finish that is smooth by taking advantage of the temperature gradient over the heating and cooling die.

3. Methodology

3.1 Setup Overview

3.1.1 Feeder winding

Before pultruding the Flax/Thermoplastic tapes, the twisted flax yarns have to first be harvested from the fibre roll and then wound onto the feeding system that will later be used for the pultrusion process. In order to wind the fibres onto the feeder, each flax yarn is tied to a designated slot on the feeder. The yarns are then passed over the splitter and threaded through guiding holes which will prevent tangling of the yarns during winding, as shown in Figure 21(b). In order to maintain tension in the yarns during the winding process, weights are hung to the ends of each yarn. The feeder is then connected to a motor which spins it and gradually winds up the fibres, resulting in the setup shown in Figure 20. As the fibres are wound, the feeder is gradually shifted closer to the splitter until all fibres have been entirely collected, as shown in Figure 21(ad). Once the yarns are fully wound, the weights can be removed, and the feeder is positioned onto the pultrusion setup, ready for the pultrusion stage.

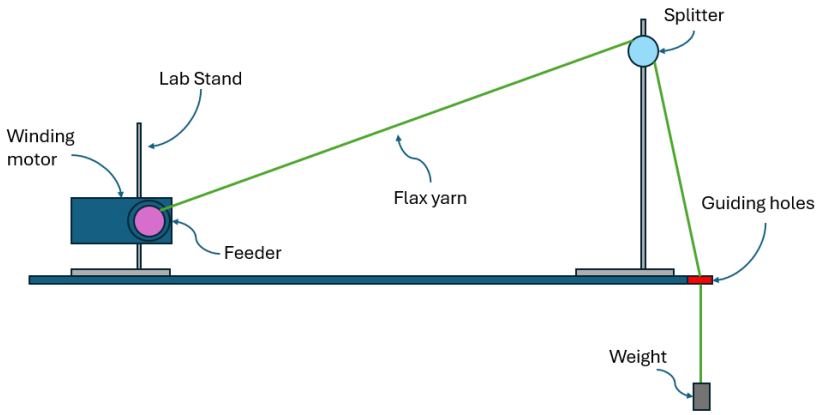

Figure 20: Diagram of the setup used to wind flax yarns on the feeder

Figure 21: (a) Flax yarns tied on the feeder slots. (b) Process of passing the yarns through the splitter and the guiding holes. (c) Start of the winding process. (d) End of the winding process, the feeder has been moved closer to the splitter in order to wind the yarns.

3.1.2 Pultrusion Setup

The pultrusion setup that was developed for this project, as shown in Figure 22 and 23, is the result of an iterative design process and it consists of five main stages: feeding, tensioning, splitting, impregnation, and winding.

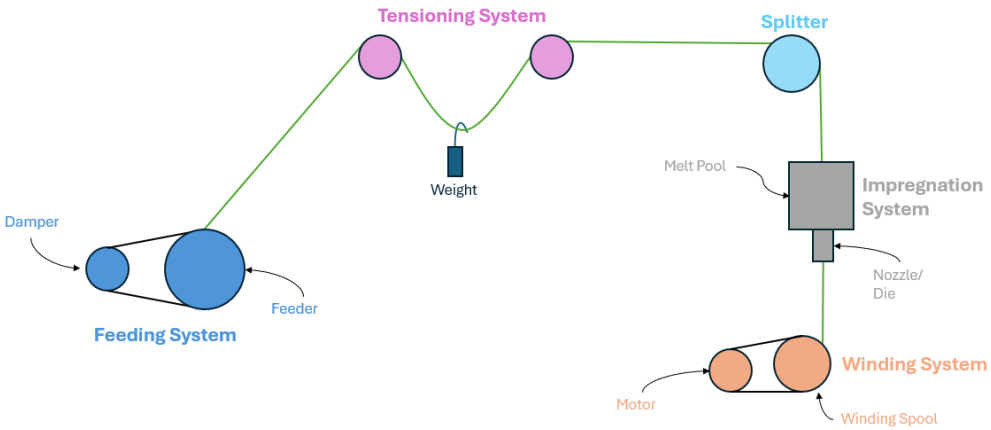

Figure 22: Diagram showing the pultrusion setup

Beginning with the feeding system, the wound yarns are positioned and connected to a rotary damper (Figure 24a). The damper is essential in regulating the feeder's rotation using friction, thus preventing free spinning of the feeder which would result in a loss of yarn tension. The yarns are then guided through a tensioning system, where small weights are attached to each yarn (Figure 24b), keeping them taut throughout the process. This tensioning helps to prevent tangling, ensuring consistency and maintaining the quality of the final product.

Following the tensioning system, the yarns enter the splitter, which keeps them all separated as they enter the impregnation system (Figure 24c). The first part of the impregnation system is the melt pool, where the melted thermoplastic is kept at a constant temperature. The melt pool is followed by an impregnation and a consolidation die which shapes the tape into the desired geometry. The finished tapes are then collected by a winding system (Figure 24d), which is powered by a stepper motor and pulls the tape out of the die at a constant speed.

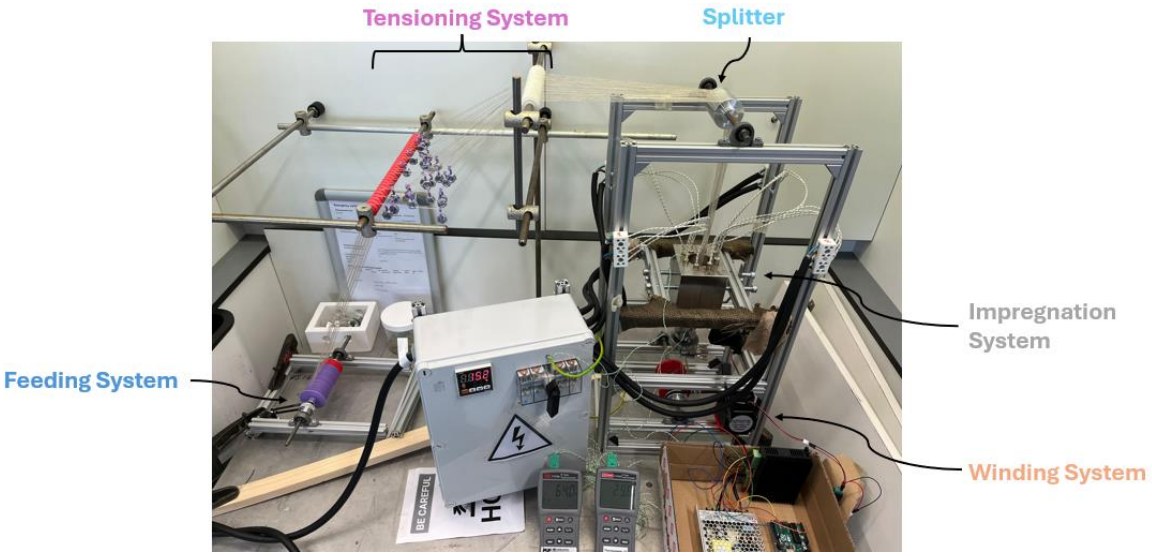

Figure 23: Photo of the pultrusion setup showing the different sections illustrated in Figure 22

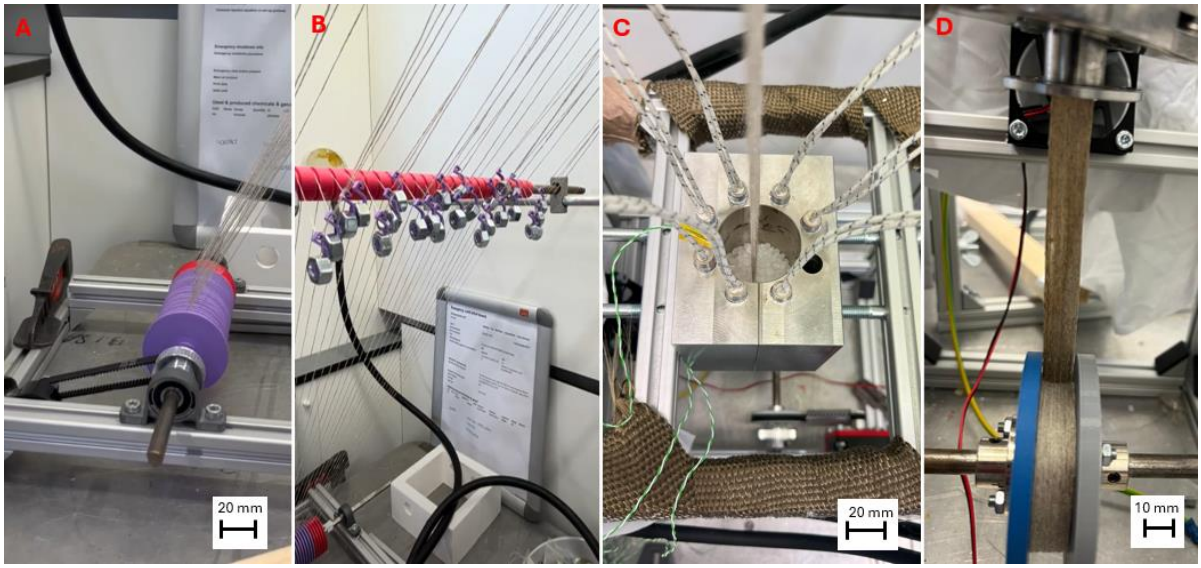

Figure 24: (a) Photo showing the damper and feeder connected by a timing belt. (b) Photo showing the tensioning system. (c) Photo from the top of the impregnation system showing the flax yarns entering the melt-pool. (d) Photo of the exit of the pultrusion die, where the winding system collects the tape.

3.1.3 Impregnation system

The impregnation stage is the most intricate part of the process, and also the focal point of the setup, where the tapes are both impregnated and consolidated inside one continuous die. This step includes a temperature-controlled melt pool, where thermoplastic pellets are melted, followed by a die which is divided into two sections: a tapered section for impregnation and a straight section for consolidation. The whole die (both the impregnation and consolidation

sections) was designed to be modular, allowing for testing of different die lengths. The yarns are first pulled through the tapered section, which narrows from 4.05 mm to 0.3 mm at a constant 4° angle, before entering the straight section, which has a continuous 0.3 mm height. Meanwhile, the die's width remains fixed at 12mm in both the tapered and straight section, as shown in Figure 25. As shown in Figure 25, the tapered die section is modular thus allowing for lengths of either 27.5 mm or 55 mm.

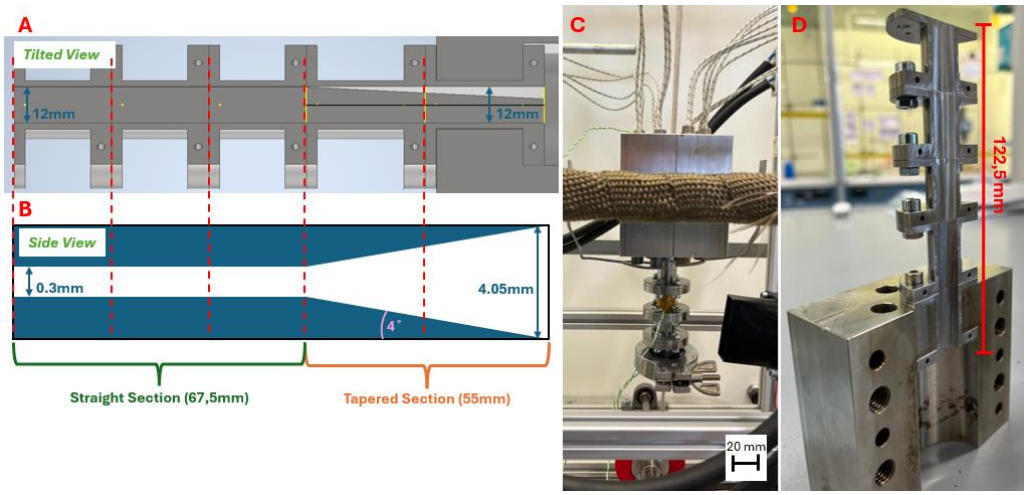

Figure 25: (a) Tilted view of one half of the die, showing the 5 sections making up the modular die. (b) Side view representing the inside of the assembled pultrusion die. (c) Photo showing the assembled impregnation system with the longest die configuration. (d) Photo showing half of the impregnation system with the longest die configuration.

When using the longer tapered die configuration (illustrated in Figure 26), the second die extends outside the heated melt pool block which inherently reduces the temperature of the second tapered die with respect to the first one. This causes the polypropylene to begin hardening prematurely. In order to mitigate this problem, a heat gun is used to keep the second tapered section heated, ensuring proper Impregnation throughout the long taper die configuration.

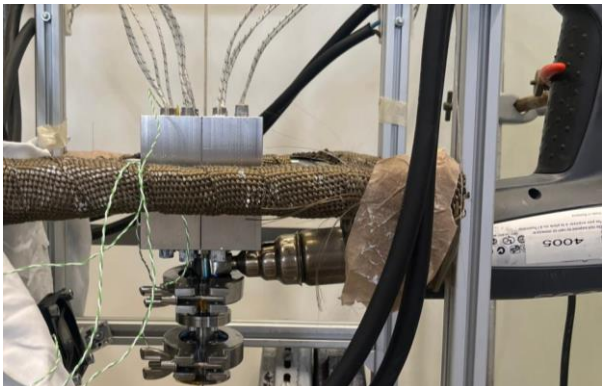

Figure 26: Photo showing the heat gun used to heat up the tapered die.

3.2 Testing Phase 1

3.2.2 Materials

The tapes are composed of two main materials:

- Reinforcement: Flax Fibre aRliTex" 300, UD by Bcomp
- Matrix: Isotactic Polypropylene with an average molecular weight (Mw) of 250,000 and an average number molecular weight (Mn) of 67,000

The tapes are manufactured using 27 flax yarns and melting 12g of polypropylene into the melt pool. The reason for choosing polypropylene originates from its balance of affordability and favourable properties, making it suitable for the development phase, where material consumption is high. In addition, polypropylene was a reasonable choice considering that the

benchmark industry sample was a flax/PP composite, which later in the research allowed for a fairer comparison. This way, as we refine the setup, we can assess how closely our output aligns with the current state-of-the-art.

3.2.3 Experimental Procedure

The first testing phase was designed as a preliminary set of experiments to understand the setup's functionality, observe the response of the flax fibres, and establish a baseline for future testing. This phase aimed to evaluate the impact of several key parameters on the quality of the composite tapes. The variables tested included:

- Melt pool temperature: 160, 170, 180, and 190°C
- Pulling speed: 30, 60, 90 mm/min
- Straight die length: 45 mm (Figure 27b) and 67.5 mm (Figure 27a)

Throughout all tests, the length of the tapered die was kept constant at 27.5 mm.

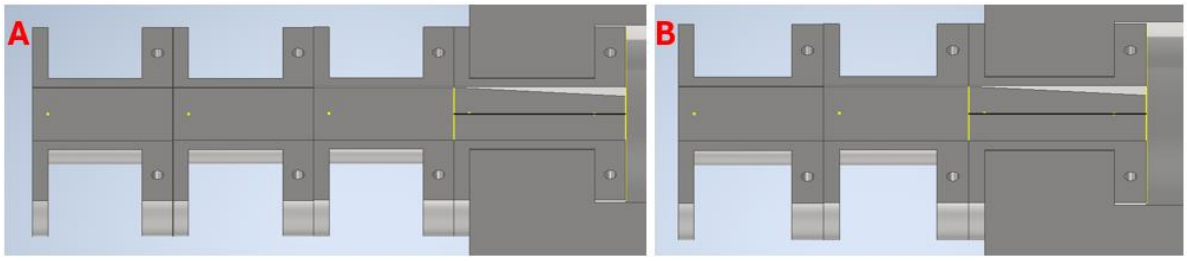

Figure 27: Tilted view of one half of the assembled die configurations used for the first testing phase.

To examine these variables, eight testing rounds (A–H, as indicated in the table below) were carried out. In all the rounds, the straight die (cooling/consolidation die) length and temperature were kept constant, but drawing speed was increased stepwise from 30 to 60 mm/min and then to 90 mm/min. A 20 cm tape sample was collected for each pulling speed to ensure uniformity. After each collection, the pulling speed was altered, and another 20 cm sample was pultruded to guarantee that the die had reached a steady state before collecting the subsequent sample.

		<----------20cm---------->			<20cm>	<----------20cm---------->			<20cm>	<----------20cm---------->		
		1				2				3		
Tape	Temp/C	Pull S. mm/min	Taper L. mm	Straight L. mm		Pull S. mm/min	Taper L. mm	Straight L. mm		Pull S. mm/min	Taper L. mm	Straight L. mm
A	160	30	27,5	67,5		60	27,5	67,5		90	27,5	67,5
B	160	30	27,5	45		60	27,5	45		90	27,5	45
C	170	30	27,5	67,5		60	27,5	67,5		90	27,5	67,5
D	170	30	27,5	45		60	27,5	45		90	27,5	45
E	180	30	27,5	67,5		60	27,5	67,5		90	27,5	67,5
F	180	30	27,5	45		60	27,5	45		90	27,5	45
G	190	30	27,5	67,5		60	27,5	67,5		90	27,5	67,5
H	190	30	27,5	45		60	27,5	45		90	27,5	45

Table 4: Table showing the 8 testing rounds (A-H) that were performed during the first testing phase.

3.2.4 Characterization

For each set of variables, the 20 cm samples were cut as shown in Figure 28 to obtain three testing samples for surface texture analysis (blue) and three for cross-sectional analysis (purple).

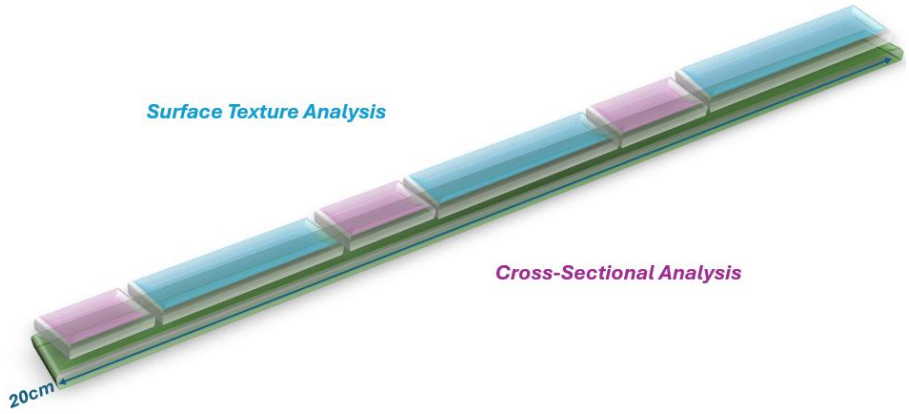

Figure 28: Illustration showing how the 20cm tape section was divided up to obtain samples for surface texture and cross-sectional (void percentage) analysis

3.2.4.1 Surface Texture

To analyse the surface texture of the samples, the Keyence VK-X1000 Laser Scanning Confocal Microscope (LSCM) was utilized. The reason for taking into account surface texture as opposed to waviness or roughness is to avoid uneven cut-off wavelengths. Because the surface texture in the same sample varies—where some regions show periodic repetition distortions (waviness) and others short-wavelength imperfections (roughness)—applying a single wavelength cut-off would yield a false reading. By taking into account only the primary profile, one does not need to constantly vary the wavelength cut-off, and a correct and comprehensive representation of the surface texture is yielded.

To examine the surface texture, the Multi-line Assessment feature of the LSCM was used with 5x magnification, using 21 perimeter lines at 50-pixel intervals. Figure 29 below shows how the multi-line assessment was carried out on each sample, repeated five times to span the entire width of the tape. As three samples were examined for every combination of variables, the average surface texture was calculated by taking the average Ra over 15 Multi-line assessments.

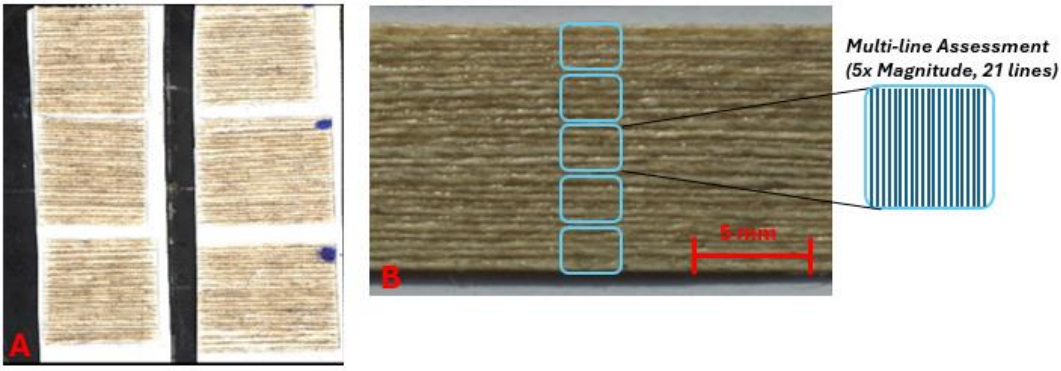

Figure 29: (a) Photo of the samples taped to the microscope plate using double-sided tape. (b) Illustration showing how the multi-line assessment was performed on each sample.

3.2.4.2 Cross-Sectional Analysis

Just as in the surface texture analysis, the cross-sections of the samples were analysed using a Laser Scanning Confocal Microscope (LSCM). The sample preparation for cross-sectional analysis involved embedding the samples in epoxy (Figure 30) and polishing them to reveal the tape structure for void percentage analysis.

After polishing and drying, the cross-sections were imaged using confocal or laser, or a combination of the two techniques, depending on the condition of the sample. The reason for using multiple techniques is that some tapes had absorbed a lot of moisture during polishing, making it difficult to capture images. Trying to dry this moisture in a vacuum oven was found to be counterproductive since the desorbed water had to be wiped off, leaving scratches on the surface.

Although the cross-sectional images could not be analysed to accurately determine percent void volumes, they were utilized to observe the geometry of the tapes and validate the observations from the surface texture measurements.

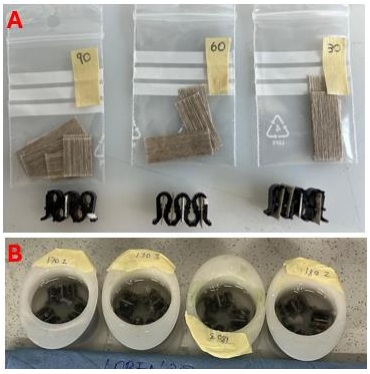

Figure 30: (a) Photo showing the nine cross-sectional samples. (b) Photo showing the embedded samples

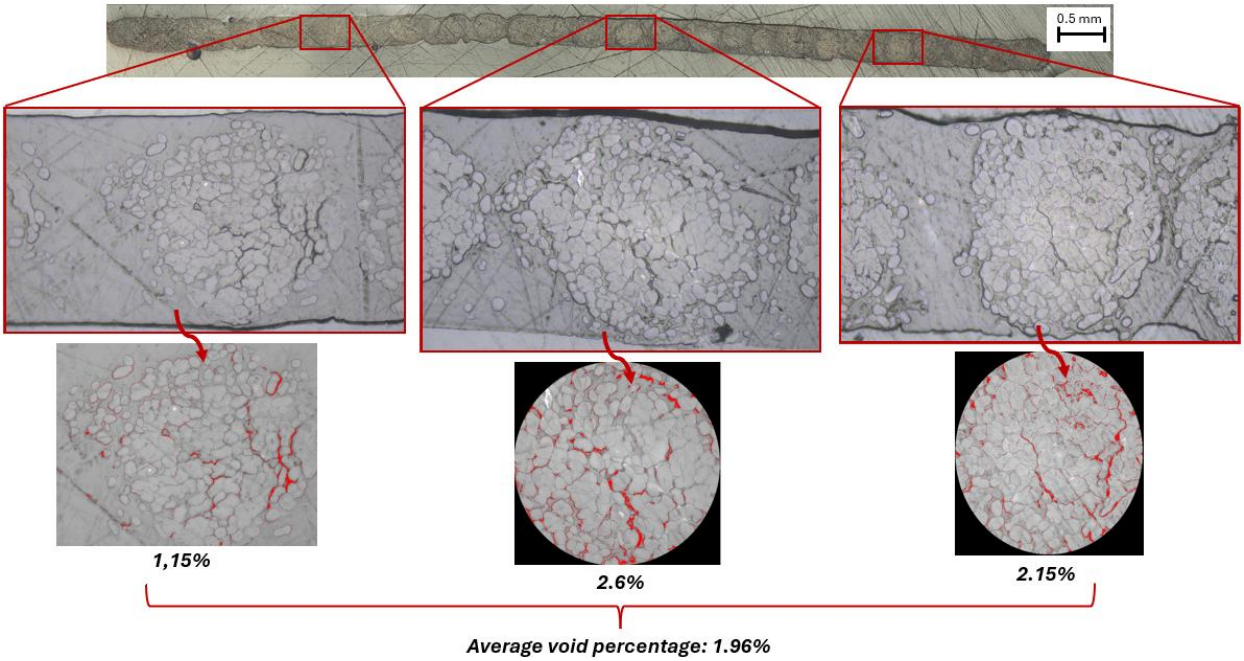

Figure 31: Diagram showing how the cross-sectional void analysis was conducted

3.2 Testing Phase 2

3.2.1 Materials

The tapes are made up of the same two materials used during the first testing phase:

- Reinforcement: Flax Fibre ampliTex™ 300, UD by Bcomp
- Matrix: Polypropylene Isotactic, average Mw 250,000, average Mn 67,000

Unlike the first testing phase, the tapes during the second testing phase were made with 30 flax yarns, with 12 g of polypropylene pellets added to the melt pool.

The tapes produced were also compared with a reference unidirectional flax/polypropylene prepreg composite tape produced by BREG, with a 50% fibre volume fraction.

3.2.2 Experimental Procedure

This testing phase was developed based on conclusions made from the initial testing phase, in order to further investigate some aspects to further enhance the quality of the tape.

Variables altered in this testing phase were:

- Melt pool temperature: 170 and 190°C
- Drawing speed: 30, 60, and 90 mm/min
- Length of tapered die: 27,5 mm (Figure 32b) and 55 mm (Figure 32a)

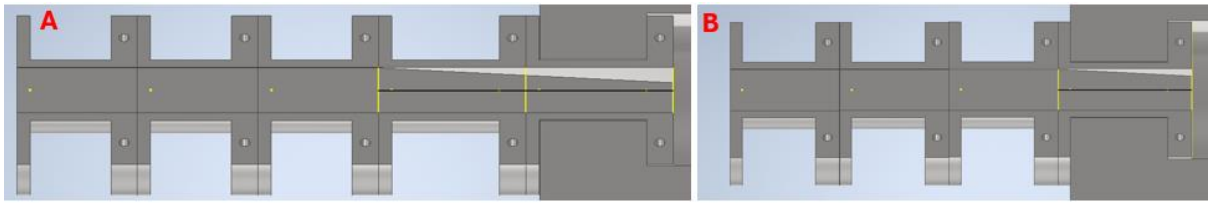

Figure 32: Tilted view of one half of the assembled die configurations used for the second testing phase

The length of the straight die was kept at constant 67.5 mm. Since the long tapered die configuration was used, heat was introduced by using a heat gun to ensure that the melt temperature was maintained through the length of the tapered die. To examine the variables mentioned above, a similar approach to the first testing phase was followed. In this case, however, four test rounds (A–D, as shown in the Table 5) were conducted. In each round, the tapered die length and temperature were kept constant, and the pulling speed was successively raised from 30 to 60 mm/min, and again to 90 mm/min. A 45 cm tape sample was collected at each pulling speed. After each collection, the rate of pulling was altered, and a 20 cm sample was created to ensure that steady state had been reached before the next sample was collected.

		<----------45cm---------->			<20cm>	<----------45cm---------->			<20cm>	<----------45cm---------->		
		1				2				3		
Tape	Temp/C	Pull S. mm/min	Taper L. mm	Straight L. mm		Pull S. mm/min	Taper L. mm	Straight L. mm		Pull S. mm/min	Taper L. mm	Straight L. mm
A	170	30	27,5	67,5		60	27,5	67,5		90	27,5	67,5
B	170	30	55	67,5		60	55	67,5		90	55	67,5
C	190	30	27,5	67,5		60	27,5	67,5		90	27,5	67,5
D	190	30	55	67,5		60	55	67,5		90	55	67,5

Table 5: Table showing the 4 testing rounds (A-H) that were performed during the second testing phase.

At the time of testing, a setup issue was discovered in the long-tapered die setup (Figure 32a). An engineering flaw prevented the die from closing in this setup, which caused the thickness of the tape to increase from approximately 0.3 mm to 0.4 mm.

3.2.3 Characterization Technique

3.2.3.1 Surface Texture

Surface texture of the tapes was analysed through the same process described for the first testing phase.

3.2.3.2 Die Exit Temperature

The temperature of the tape upon exit from the die is important as it bears a relation to the consolidation level of the tape. The exit temperature also allows one to calculate the cooling rate of the tape in the die, which is utilized in the estimation of the crystallinity level of the sample.

In order to track the temperature of the tape, an IR Camera (FLIR A615) was focused on the die exit and images were taken to capture the temperature. A sample of the obtained results from the use of the IR camera is presented in Figure 33 below.

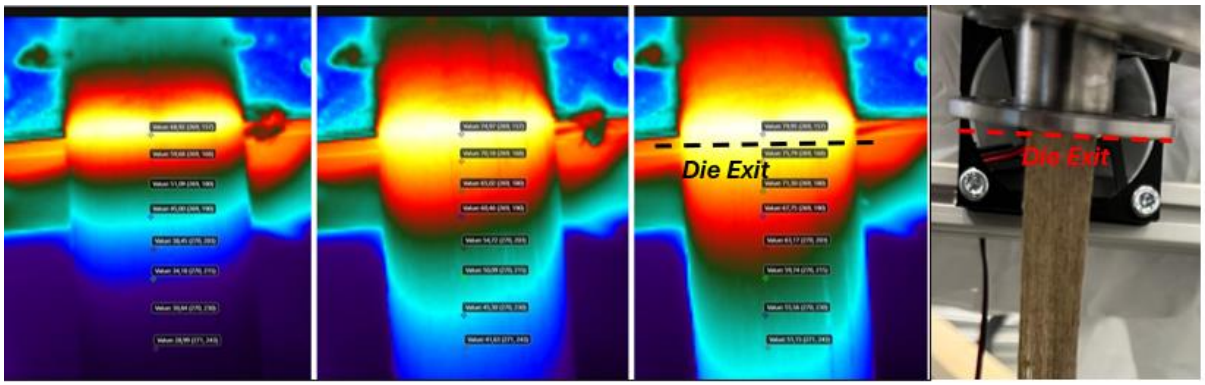

Figure 33: Three images obtained with the FLIR A615 camera, showing the exit temperature of the composite tape at different pulling speeds. The photo on the right shows where the camera was pointed at.

3.2.3.3 Cross-Sectional Analysis

Unlike testing phase 1, MicroCT was used in examining the cross-section of the tape (Figure 34a). The advantage of using MicroCT compared to LSCM is that it omits a polishing step, which wets the fibres and complicates the analysis.

The MicroCT cross-sectional images were processed using the Threshold function in ImageJ to estimate the void and fibre percentage (Figure 34). It must be noted here that the images obtained by MicroCT are of relatively poor quality (highly pixelated), and it is hard to obtain very precise void percentage results. As can be seen in Figure 34b,c, the same image can provide 2.5 % or 4.32 % void percentages, which leaves some subjectivity to the individual analysing the images.

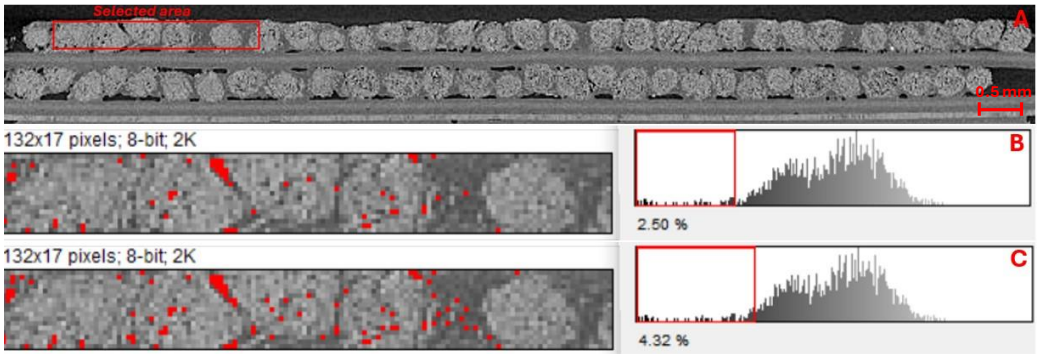

Figure 34: (a) MicroCT image of two full cross-sections on top of each other, as obtained from the machine. (b,c) Pictures of the selected area from image 'a' with different thresholds applied to them, yielding different for void percentage

Void and fibre volume percentages were calculated by selecting a single tape cross-section for each combination of variables on ImageJ and applying two thresholds: one to define the voids and one to define the yarns, as seen in Figure 35.

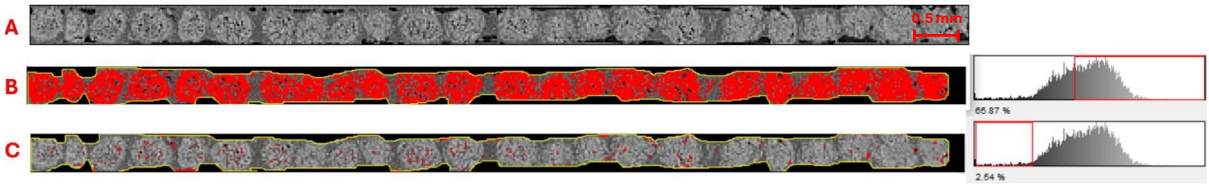

Figure 35: Three screenshots taken from the ImageJ environment showing the original cross-section (a) and illustrating how the fibre yarns (b) and voids (c) were highlighted to estimate their volume percentage

3.2.3.4 Tape Thickness

The thickness of the tapes was measured from the MicroCT cross-sectional images using the 'Measure' tool on ImageJ. Five equally spaced measurements along the tape width were taken for each set of variables as shown in Figure 36. The average thickness for the sample was taken as the mean of the 5 measurements. The thickness of the samples prepared with the short die configuration was compared with that of samples prepared with the long die configuration to investigate the influence of changing die geometries on the overall thickness of the tapes.

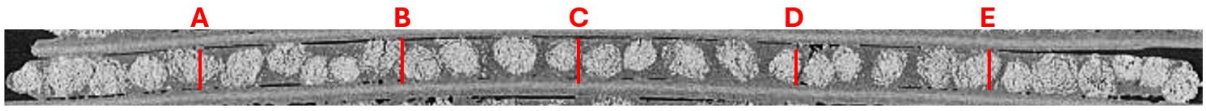

Figure 36: Illustration of how the thickness measurements were taken

3.2.3.5 Lap Shear test of Ultrasonic-Welded samples

In the case of thermoplastic composite materials, particularly composite tapes, ultrasonic welding (USW) is an attractive technique for quickly testing layer adhesion. The simplicity of the setup makes it possible to prepare multiple samples for single lap shear testing, allowing the potential of the produced tapes to be evaluated. Moreover, compared to tape laying, USW permits welding of small-scale samples, which is beneficial in the case of this project. Although the main objective of this thesis is to produce composite tapes for tape laying, USW was used to produce lap shear samples, providing a rapid method to test the strength and adhesive qualities of the tapes. In addition to welding the pultruded tapes, BPREG benchmark composite tapes were also welded and tested to compare their adhesive qualities with the pultruded tapes.

The lap shear samples were made using ultrasonic welding (USW) with 300 N weld force, 0.650 s weld time and 66 % amplitude (30 µm nominal amplitude). Two strips of composite tape 8 cm long were welded together for each lap shear sample, and the welding area was chosen according to lap shear ASTMD5868 standard for fibre-reinforced plastics, which is 12,7 mm (1 in) x 12 mm (Figure 37a,b shows the weld ready for use). In addition, no energy director was utilized in welding to ensure that the weld quality didn't depend primarily on the energy director. Instead, the aim was to see how the processing temperature and surface roughness affected the weld quality of the tapes.

Once the samples were welded, they were transferred to a universal tensile machine fitted with a 10 kN load cell. For lap shear testing, since the samples were 0.3-0.4 mm thick and would easily slip out of the clamp, two aluminum plates were placed as indicated on Figure 37d, to facilitate proper clamping of the samples. Clamp distance was 5 cm and crosshead speed was 1.3 mm/min according to ASTM D3163 standard. Two lap shear tests for each set of variables were carried out and the results were plotted on *Force(N)* vs *Strain(mm)* charts. The elongation and stress at break were measured.

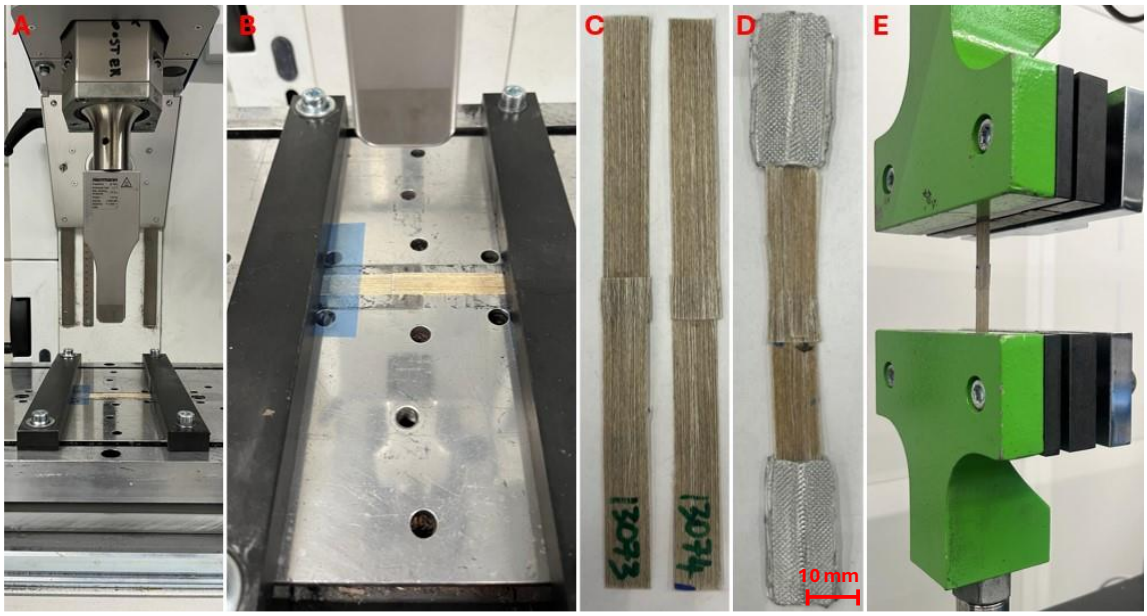

Figure 37: (a,b) Photos of the flax tapes clamped down in the ultrasonic welding machine. (c) Photo of two ultrasonic welded samples before testing. (d) Photo of an ultrasonic welded sample with aluminium supports on the extremities, to ensure good clamping in the tensile machine. (e) USW sample placed in the tensile machine

4. Results and Discussion

4.1 Testing Phase 1

4.1.1 Results

4.1.1.1 Surface Texture

Firstly, from the results of the long straight die setup in (Figure 38, Table 6) it is evident that the melt pool temperature of 170°C was the one which produced samples with the minimum surface texture, regardless of the pulling speed. In contrast, samples pulled at melt pool temperatures of 160°C, 180°C, and 190°C had significantly higher surface texture values. It is difficult to delineate sharp trends as far as pulling speed at these three temperatures, because their surface texture values are relatively similar and fall within one another's standard deviation.

For the short straight die design (Figure 38, Table 7), surface texture values show a clear dependence on both temperature and pulling speed. This is particularly noticeable at 180°C and 190°C, where the surface texture values at 190°C are consistently 3-4 µm greater than those at 180°C regardless of pulling speed. Furthermore, the rise in the pulling speed is accompanied by a consistent rise in the surface texture in samples pulled from both 180°C and 190°C. In contrast, samples pulled at 170°C possessed virtually constant values for surface texture that were not dependent on the changes in pulling speed. Besides, for all temperatures, samples made with the short die setup consistently had higher standard deviation values than those made with the long die setup, which had more variability in the data.

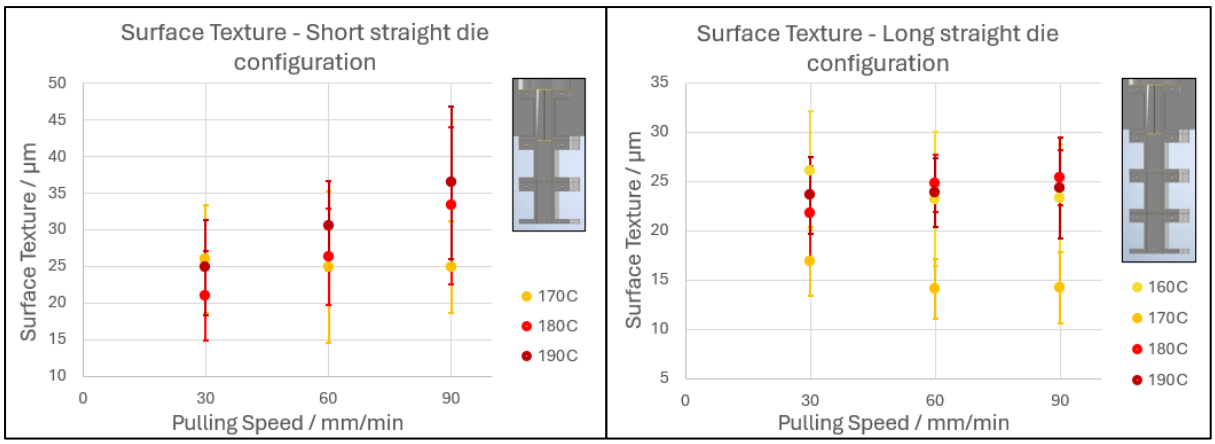

Figure 38: The graph on the left illustrates the surface texture vs pulling speed for the short straight die configuration, while the right one shows it for the long straight die configuration

Puling Speed (mm/min)	160˚C		170˚C		180˚C		190˚C	
	Texture / µm	Stdev	Texture / µm	Stdev	Texture / µm	Stdev	Texture / µm	Stdev
30	26,1	6,0	16,9	3,5	21,8	4,7	23,6	3,9
60	23,2	6,8	14,1	3,0	24,8	2,9	23,9	3,5
90	23,3	5,4	14,2	3,6	25,4	2,8	24,4	5,1

Table 6: Table of the surface texture results from the long straight die configuration

Puling Speed (mm/min)	170˚C		180˚C		190˚C	
	Texture / µm	Stdev	Texture / µm	Stdev	Texture / µm	Stdev
30	26,1	7,4	21,1	6,1	24,9	6,5
60	25,0	10,3	26,3	6,6	30,6	6,1
90	25,0	6,3	33,3	10,7	36,5	10,4

Table 7: Table of the surface texture results from the short straight die configuration

4.1.1.2 Cross-Sectional Analysis

The hydrophilic character of flax caused it to swell with large amounts of water during grinding and polishing operations involved in sample preparation. This swelling was noticeable when examining under the microscope, hence, to alleviate this, polished samples were dried in a 60°C vacuum oven for 3 hours to desorb water. The water, though, could be removed from the surface only by wiping, which produced numerous scratch marks on the samples. Therefore, not all the water could be evacuated, and scratch marks made it impossible to properly analyse the tape cross-sections using the microscope.

Therefore, it was not possible to carry out a valid void and fibre volume percentage analysis. However, when looking at some of the few clear photographs of the 170, 180 and 190°C samples, there are no visible or consistent differences in void percentage between the samples (Figures 39, 40 and 41).

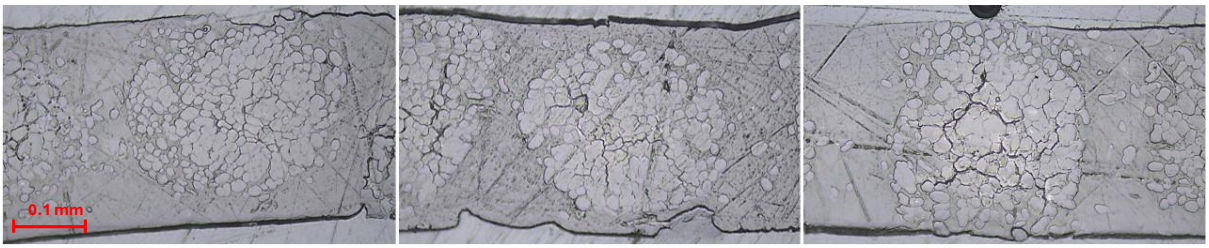

Figure 39: Three cross-sectional images of the samples produced at 170°C with long straight die configuration

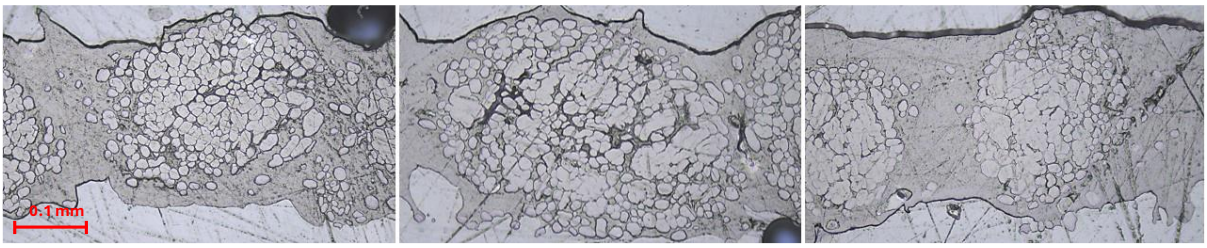

Figure 40: Three cross-sectional images of the samples produced at 180°C with long straight die configuration

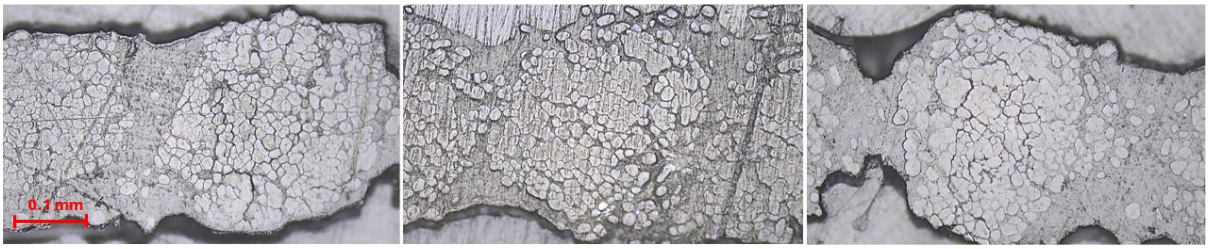

Figure 41: Three cross-sectional images of the samples produced at 190°C with long straight die configuration

In contrast to the samples made at 170°C, 180°C, and 190°C, those treated at 160°C had clearly larger voids. While most samples still exhibited some fibre swelling even after the drying step, this phenomenon was much more evident in the 160°C samples. This is likely due to lower impregnation at this temperature, which made the fibres even more water-sensitive. Evidence of such water swelling can be seen from Figure 42 below, where some water droplets are seen, and in some areas, bundles of fibres are difficult to distinguish because of widespread swelling.

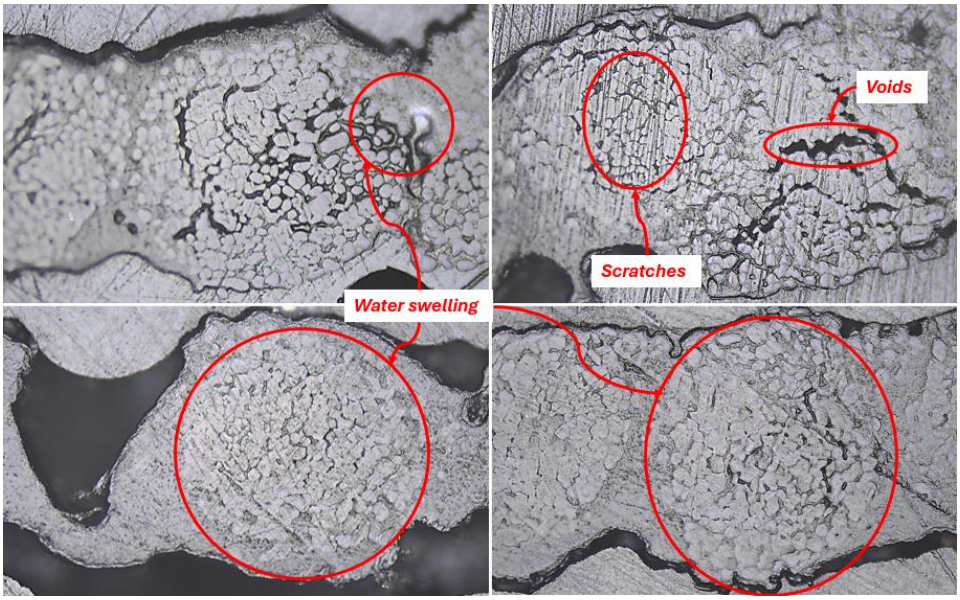

Figure 42: Sections from the cross-sectional images of the 160C samples. Here some features were highlighted to show the swollen fibres, scratches and voids.

Although the cross-sectional analysis failed to give results for void percentage analysis, it gave satisfactory visual confirmation of the surface texture analysis results. The surface texture analysis indicated that the lowest surface texture was obtained in samples produced at 170°C using the long straight die (Figure 44). The same can be confirmed by the cross-section of the sample, which shows a smooth top and bottom surfaces. The space between the round yarns appears to be filled in, rather than following the periodic waviness of the yarns, resulting in a relatively smooth and flat surface compared to other samples (Figure 45). The higher surface roughness of short die configuration specimens was also confirmed by the cross-sectional analysis as given in Figure 43 below.

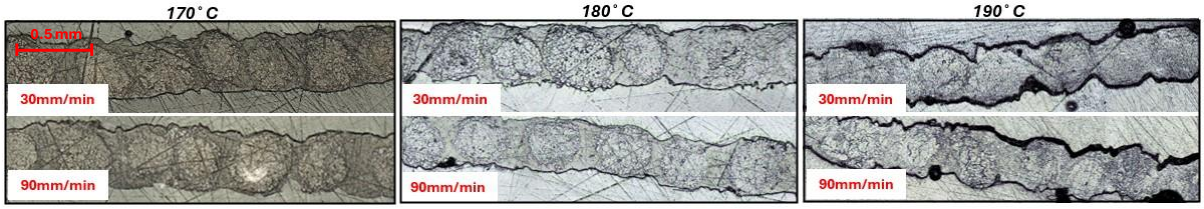

Figure 43: Cross-sectional images of the samples from the short straight die configuration at 30 and 90mm/min

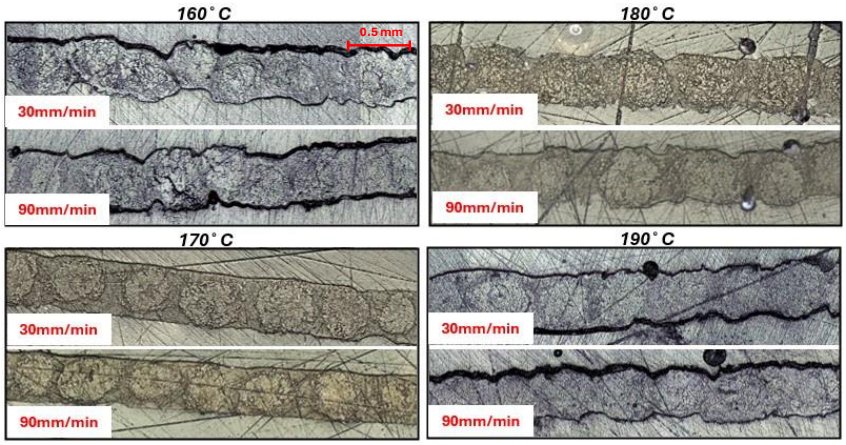

Figure 44: Cross-sectional images of the samples from the long straight die configuration at 30 and 90mm/min

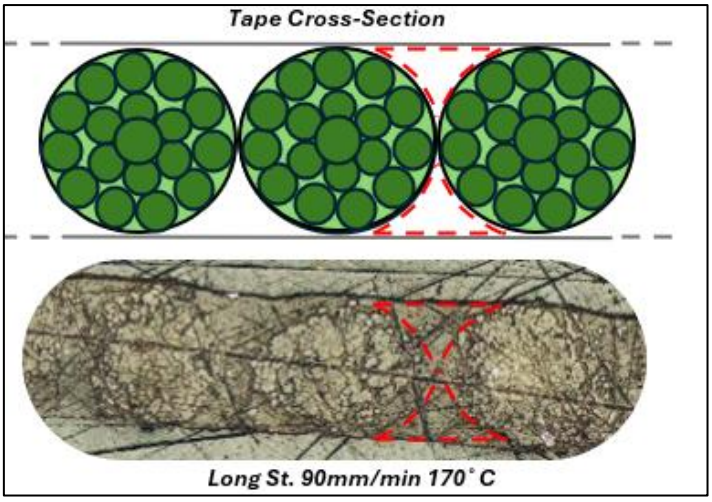

Figure 45: Illustration to show how the samples at 170C were able to fill the gaps (highlighted in red) between the yarns

4.1.2 Discussion

This first testing phase led to several findings which were essential to better understand the setup and the behaviour of the tapes. One of the key findings was that the long straight die setup had the tendency to produce samples of better quality compared to the short straight die setup. This is most likely because of the longer residence time in the die, which allows for better consolidation of the tape before exiting. The limited consolidation time in the short die, leads to less fixation of the yarns in the thermoplastic matrix, which are likely to relax and cause higher surface texture.

Another observation was the effect of pulling speed in the short-tapered die arrangement for samples processed at 180°C and 190°C. The trend for increased surface texture with increasing pulling speeds can be due to reduced residence time and occurrence of sloughing—when interfacial adhesion forces between polymer and metal in the pultrusion die exceed pultrudate strength. This adhesion can cause fragments to stick to the die surface and be ripped off from the tape, deteriorating its surface quality. The sloughing effect is more apparent at the higher pulling speeds because the tape does not have sufficient time to cool and 'detach' from the metal walls as it is being pulled through the die at a higher speed.

Cross-section examination also revealed that samples drawn at 170°C using the long straight die configuration had significantly less surface texture. This was due to the fact that the matrix occupied areas between yarns (marked in red in Figure 41), effectively reducing surface height deviations. In contrast, samples produced at 160°C and at 180°C/190°C overall did not fill these gaps. For the samples produced at 160°C, the high viscosity of the resin (close to its melting point) likely inhibited shearing of the polymer into the die cavity and hence led to poor impregnation and prevented the resin from flowing transversely into the fibre yarns. On the other hand, for the samples produced at 180°C and 190°C, the lowered viscosity likely resulted in a certain degree of resin backflow at the exit of the tapered die. This backflow reduced mechanical shearing in the narrow straight die area, causing the polymer to flow backward rather than occupying the void between the flax yarns.

In addition, the majority of the samples had visible gaps between yarns due to lack of fibre contact. The size of these gaps could be lowered with an increased number of yarns, which would reduce the backflow effect and potentially result in better surface texture for tapes processed at 180°C and 190°C.

In line with these results, a second test phase was carried out for the optimization of the tapes. This phase was concerned with melt pool temperatures of 170°C and 190°C—170°C due to its superior performance in the previous phase, and 190°C to determine if backflow effects could be minimized by raising the yarn count. The influence of changing the length of the tapered section was also investigated, with the straight die length kept at 67.5 mm, which had yielded the best results previously. Lastly, in recognition of the limitations of embedding and polishing for cross-sectional void and fibre analysis, a new characterisation method was presented to improve the accuracy of measurements.

4.2 Testing Phase 2

4.2.1 Results

4.2.1.1 Surface Texture

The first analysis for the second testing phase was the evaluation of the surface texture. Overall, the texture of samples made with the long-tapered die configuration was found to be lower than those made using the short-tapered die, as seen in Figure 46 and Table 8. Surface texture results for samples made in the short taper configuration, which was also tried in the first phase, were similar to earlier work for samples made at 170°C, whereas samples made at 190°C showed a considerable decrease in surface texture. Furthermore, surface texture increased for 170°C and 190°C samples with an increase of pulling speed. However, since these results have high standard deviations, increasing the batch size might provide more accurate and consistent results to draw appropriate conclusions.

For the long-tapered die configuration, the same trend was also seen, where surface texture grew with increasing pulling speeds. Again, as with the short taper configuration, the large standard deviations indicate that increasing the sample size would probably increase the precision of the results

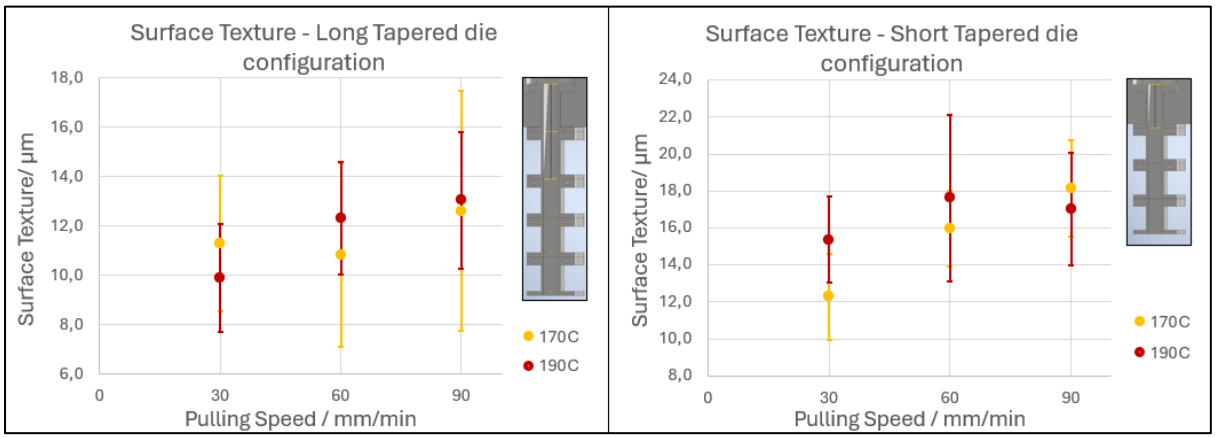

Figure 46: the graph on the right illustrates the surface texture vs pulling speed for the short-tapered die configuration, while the left one shows it for the long-tapered die configuration

	170 ˚C				190 ˚C			
Puling Speed (mm/min)	Short Taper		Long Taper		Short Taper		Long Taper	
	Texture/µm	Stdev	Texture/µm	Stdev	Texture/µm	Stdev	Texture/µm	Stdev
30	12,3	2,3	11,3	2,8	15,4	2,3	9,9	2,2
60	16,0	2,0	10,8	3,7	17,6	4,5	12,3	2,3
90	18,1	2,6	12,6	4,9	17,0	3,0	13,1	2,8

Table 8: Table of the surface texture results from the short and long tapered die configuration

4.2.1.2 Die-Exit Temperature

For melt pool temperatures of both 170°C and 190°C, the outlet temperature (Tout) increases with the increase in the pulling speed from 30 mm/min to 90 mm/min for both short taper and long taper configurations (Table 9). The 190°C melt pool, as expected, always registers higher outlet temperatures than the 170°C melt pool due to its higher initial temperature. In addition, tapes manufactured with the short taper configuration experience higher exit temperatures than tapes made in the long taper configuration, most likely due to the lower die residence time in the short taper setup.

	170 ˚C		190 ˚C	
Puling Speed (mm/min)	Short Taper	Long Taper	Short Taper	Long Taper
	Tout/ ˚C	Tout/ ˚C	Tout/ ˚C	Tout/ ˚C
30	69,0	54,2	70,9	55,4
60	72,0	58,7	76,3	58,7
90	76,2	60,1	81,2	62,2

Table 9: Table of the tape temperature at the exit of the die, for different die configurations, melt-pool temperatures and pulling speeds

The cooling rates illustrated in Table 10 show a consistent pattern for both pulling speed and taper configuration. With the rise of pulling speed from 30 mm/min to 90 mm/min, cooling rate increases significantly in all conditions and melt pool temperatures. In the short taper configuration at 170°C, the cooling rate rises from 43.3°C/min when the pulling speed is 30 mm/min to 127.7°C/min when the pulling speed is 90 mm/min. Also, the cooling rates are always greater in the short taper setup than in the long taper setup, again presumably because of the reduced residence time in the shorter die, which leaves less time for heat dissipation before the tape exits.

Configuration	170 ˚C				190 ˚C			
	Speed (mm/min)	Distance (mm)	Tout ˚C	Cooling rate (˚C/min)	Speed (mm/min)	Distance (mm)	Tout ˚C	Cooling rate (˚C/min)
Short taper	30	70	69	43,3	30	70	70,9	51,4
	60	70	72	84,4	60	70	76,3	97,5
	90	70	76,2	127,7	90	70	81,2	139,9
Long taper	30	97,5	54,2	35	30	97,5	55,4	41,4
	60	97,5	58,7	68,4	60	97,5	58,7	80,8
	90	97,5	60,1	101,5	90	97,5	62,2	118

Table 10: Table of the cooling rates fir different die configurations, melt-pool temperatures and pulling speeds

4.2.1.3 Tape Thickness

The height of the tape (thickness) is greater for the long taper compared to the short taper, at both 170°C and 190°C temperatures as can be seen from Table 11. The long taper has a tape height of

428 µm, whereas the short taper has an average tape thickness of 352 µm at 170°C. Similarly, the long taper is 429 µm high at 190°C compared to 365 µm for the short taper.

170 °C				190 °C			
Short Taper		Long Taper		Short Taper		Long Taper	
Height /µm	Stdev	Height /µm	Stdev	Height /µm	Stdev	Height /µm	Stdev
352	37,006	428	42,191	365	23,609	429	34,04

Table 11: Table showing the tape thicknesses (Height) for different die configurations and melt-pool temperatures

Standard deviation values reflect more variability in tape thickness for the long taper configurations at the two temperatures, with the greatest difference at 170°C (42.191 µm). The short taper configurations are more consistent, as at 190°C the standard deviation is relatively low (23.609 µm).

4.2.1.4 Cross-Sectional Analysis

The data, as portrayed in Figure 47 and Table 12 below, shows the void and fibre volume percentages for samples produced at varying pulling speeds and melt pool temperatures, using both short and long taper configurations. For parts produced at 170°C, one can observe a higher void percentage compared to those produced at 190°C, especially in short taper configuration with 2.5% of void content when pulled at 90 mm/min. Fibre percentages are always reduced for long taper samples, likely due to the fact that the long taper configuration produces thicker tapes due to the aforementioned design flaw. Since the same amount of yarn is used in both configurations, the increased thickness in the long taper configuration automatically reduces the fibre volume percentage.

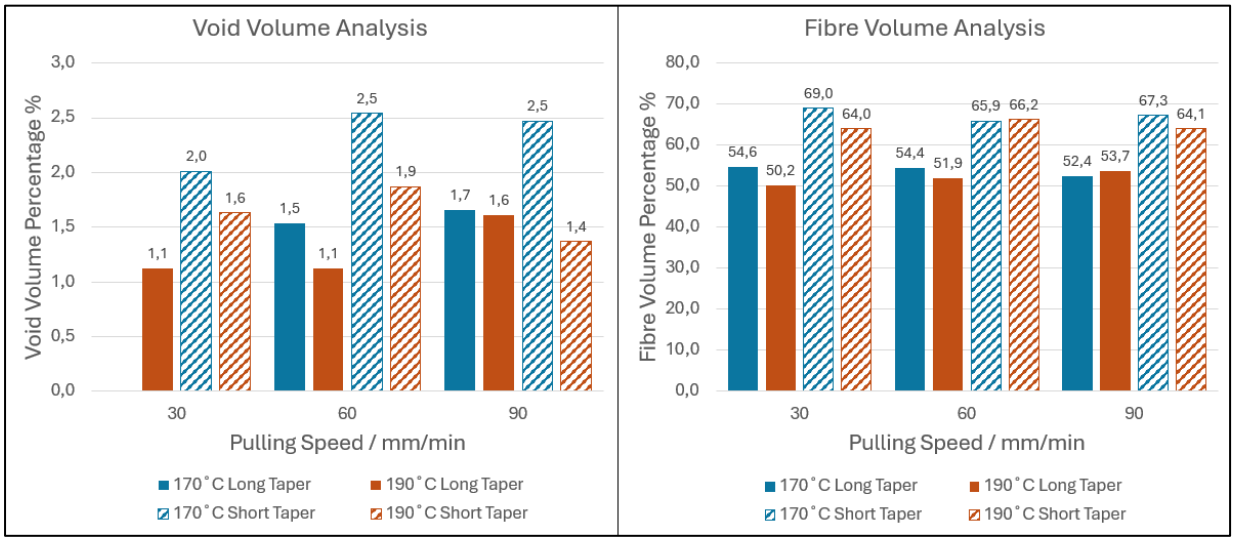

Figure 47: Void and Fibre Volume percentages obtained from the image analysis

Configuration	Pulling Speed (mm/min)	170 °C		190 °C	
		void %	fibre %	void %	fibre %
Short Taper	30	2,0	69,0	1,6	64,0
	60	2,5	65,9	1,9	66,2
	90	2,5	67,3	1,4	64,1
Long Taper	30	-	54,6	1,1	50,2
	60	1,5	54,4	1,1	51,9
	90	1,7	52,4	1,6	53,7

Table 12: Table showing the void and fibre volume percentage for different die configurations, melt-pool temperatures and pulling speeds

4.2.1.5 Lap Shear test of Ultrasonic-Welded samples

The results of the lap-shear testing are shown in Figure 48, with the orange curves (190°C samples) possessing a more abrupt initial slope than the blue curves (170°C samples), indicating tapes pultruded at higher processing temperature are stiffer. In addition, the orange curves possess greater lap shear strength overall than the blue curves. The increased levels of total stress, sustained over a greater range of displacement, reflect that the samples processed at 190°C have a better bonded sample which can withstand greater loads before failure. Particularly, the 190°C short taper setup achieves an average value of 6.5 MPa for break stress, a maximum among all setups, indicating the higher bonding and mechanical strengths at this higher processing temperature.

In comparison, the reference samples by BPREG (in green), exhibited considerably lower stress at break, between 2.3 and 2.5 N, highlighting the better performance of the samples made using the pultrusion setup.

Looking at the tested samples, only one sample failed at the weld zone, and this was a 190C samples produced at a pulling speed of 90mm/min. All the other samples either broke near the clamp as in Figure 48a or broke near the clamp and the failure propagated as an inter-yarn failure down to the ultrasonic welded area as shown in Figure 48b.

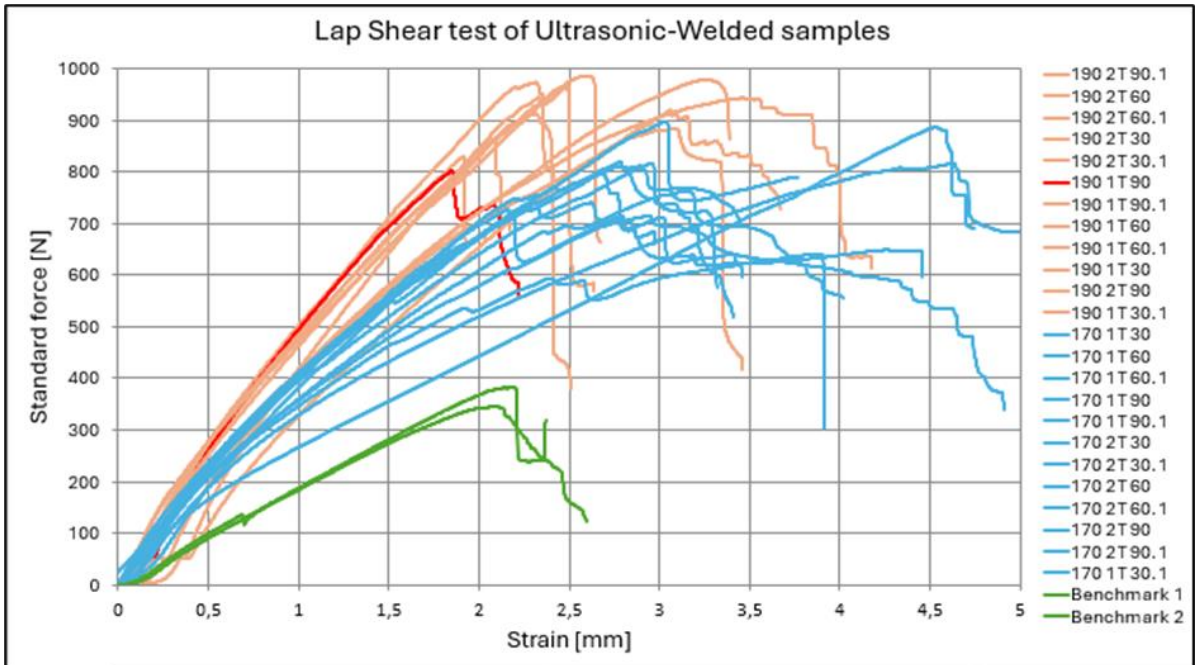

	170˚C				190˚C				Benchmark
Speed	Short Taper		Long Taper		Short Taper		Long Taper		
(mm/min)	Stress at Break/Mpa		Stress at Break/Mpa		Stress at Break/Mpa		Stress at Break/Mpa		Stress at Break/N
30	5,0	4,9	4,2	5,4	6,0	6,5	5,4	5,3	2,3
60	5,8	5,4	5,3	5,9	5,8	6,3	6,2	6,4	2,5
90	4,6	5,2	4,8	5,4	6,4	6,0	5,7	6,3	
Average	5,2		5,2		6,2		5,9		2,4

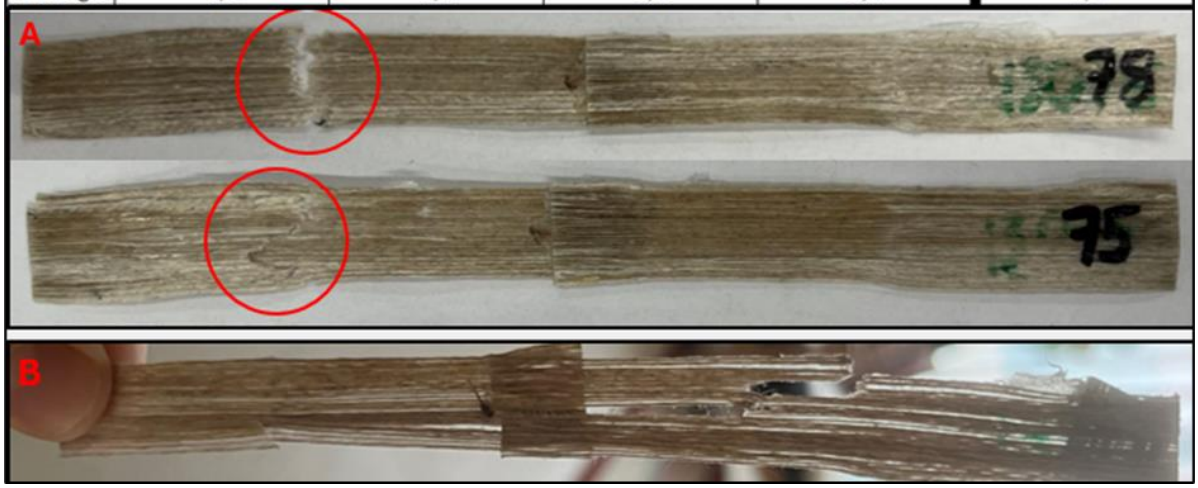

Figure 48: The graph displays all the lap shear tests, with the samples categorized by manufacturing temperature: 170°C (blue) and 190°C (red). The table below summarizes the results and provides the average stress at break for each group. Image (a) illustrates a break occurring at the clamp, while Image (b) shows a break at the clamp that propagated to the welded area.

4.2.2 Discussion

In discussing the result of the second test phase, starting with surface texture, the long-tapered die configuration produced samples with a smoother surface texture than the short taper, most likely because of several reasons. First, the longer die provides a longer residence time for the tape, allowing better surface consolidation. This provides an exit temperature, as can be seen from the temperature details, which helps in achieving smoother texture. Furthermore, the long

taper configuration tapes were thicker, because the design fault in the dies caused excess polymer to collect onto top and bottom faces, thus creating resin rich areas. The excess polymer was more likely to hold back the fibres from protruding beyond the surface which led to an overall decrease the surface texture.

Both 170°C and 190°C samples exhibited a rougher surface texture with higher pulling speeds. Consistent with the first test phase observation, the samples pulled at 90 mm/min exhibited the largest surface texture, due again to the sloughing effect as previously discussed. In contrast, at 30 mm/min, a different challenge was observed, particularly with the long-tapered die design. At 190°C, the longer residence time appeared to burn the flax, as seen by the darker shade of the 30 mm/min tape in Figure 49 below.

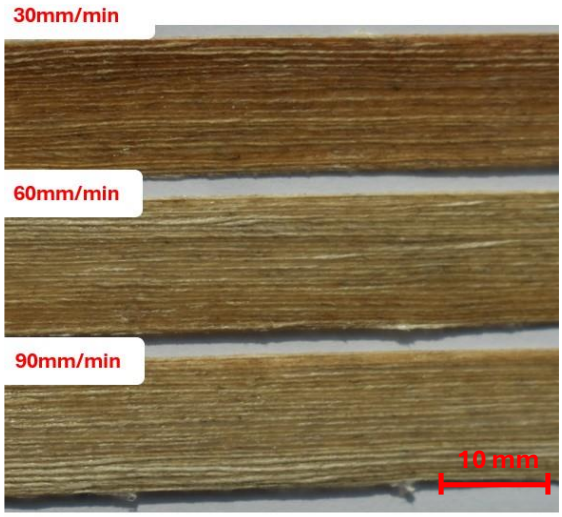

Figure 49: The image shows samples produced using the long-tapered die configuration at 190°C, tested at three different pulling speeds.

The short taper setup showed a higher fibre percentage (about 65-70%) compared to the long taper (about 50-55%). This is comparable directly with the thicker tape size that is produced by the long-tapered die. The increased thickness corresponds to an increased volume of polymer, reducing the overall fibre volume percentage by around 10-15%. In general, it is impossible to state if the long taper die configuration itself had a visible influence on the tapes, or if the differences between the short and long taper were to a significant extent governed by the increased tape thickness.

The lap shear results indicate that the samples processed at 190°C possess higher lap shear strength and stiffness than samples processed at 170°C. This difference in performance is attributed to differences in the extent of crystallinity of the polymer due to thermoplastic processing operations such as melting, shearing, and cooling. The strength and stiffness of thermoplastics like polypropylene are typically controlled by crystallinity to a large degree, with higher crystallinity tending to equate to higher strength and stiffness. In this setup, the final extent of crystallinity will be highly dependent on the polymer's cooling rate and shear rate during the cooling phase.

Crystallization of thermoplastics (like polypropylene) is extremely dependent on cooling rate. Based on a study by Hu et al., the crystallinity of polypropylene decreases at the higher cooling rate and stabilizes at over 200 K/s [54]. For parts produced at temperatures of 170°C and 190°C using different die geometries, the measured cooling rates ranged from 0.583 K/s to 2.33 K/s. According to Hu's model, these rates are seen to correspond to a degree of crystallinity greater than 95% (As indicated in Figure 50), suggesting that cooling rate cannot explain the enhanced strength and stiffness observed in the 190°C samples. Also, since the samples at 190°C have a higher cooling rate than those at 170°C, we should expect lower crystallinity, and hence lower strength and stiffness for the 190°C samples if cooling rate was the only controlling factor.

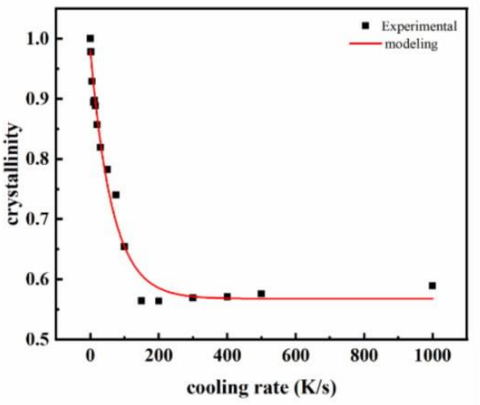

Figure 50: The relationship between crystallinity and cooling rate of PP [54]

Besides cooling rate, another factor controlling the crystallization of thermoplastics is shear rate upon cooling. In fact, shear promotes the formation of crystallization nuclei and advances crystal growth in the direction of shearing. Experiments conducted by Moitzi et al. showed that even minimal shearing significantly accelerates crystallization, particularly when employed in the case of polypropylene at around 130-135°C (Figure 51). At shear rates of $4s^{-1}$ or $12s^{-1}$, crystallization occurs rapidly, unlike quiescent polypropylene, which begins to crystallize after around one hour [55].

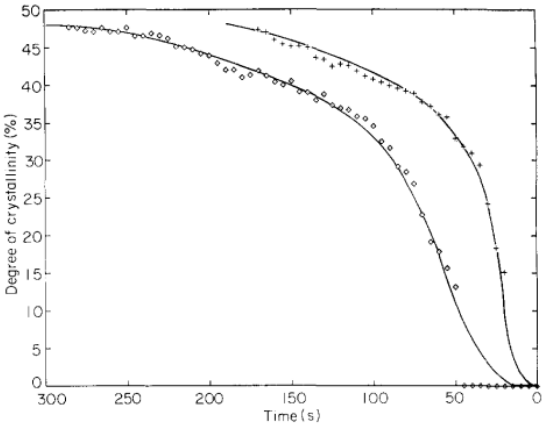

Figure 51: Degree of crystallinity versus measuring time at shearing rates of O, 4 s^{-1} and +, 12 s^{-1} for PP. Crystallization temperature 130°C [55]

Since the variables that affect shear rate are pulling speed and die geometry, the samples pultruded at 90 mm/min would be expected to experience the highest shear rate. Theoretical application of shear-induced crystallization should result in higher strength and stiffness along the direction of pulling. However, this trend is not strictly obeyed by the results, so the shear induced organization cannot be the only reason for the variation in lap shear results.

Neither the shear rate nor the cooling rate varied significantly throughout the samples tested to display clear trends in the lap shear results. Differential scanning calorimetry (DSC) examination of the virgin polypropylene pellets showed that 170°C is precisely the endset temperature of the melting curve, as can be seen in Figure 52. This is the temperature where the crystalline form of the thermoplastic melts entirely, theoretically transforming the polymer into an entirely amorphous state. Thus, we would expect there to be no crystalline phase remaining in the molten state in both the 170°C and 190°C samples.

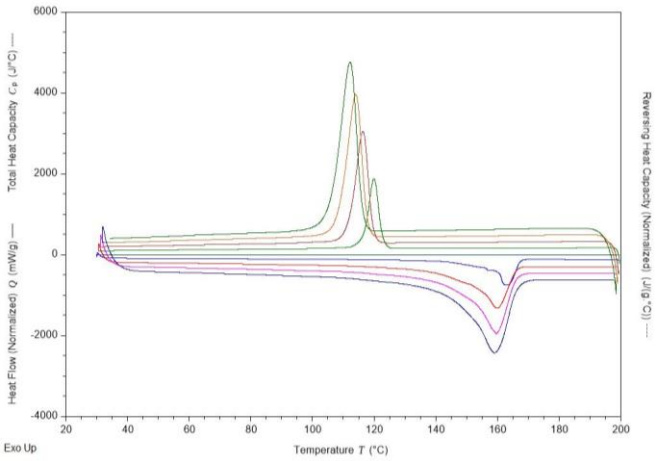

Figure 52: DSC of isotactic polypropylene used for tape pultrusion

However, it is worth mentioning that the temperature of the melted polymer was controlled by a thermocouple on the wall of the melt pool, and the temperature set was assumed to be equal throughout the pool. Because the melt pool was open and shallow (approx. 1-1.5 cm) to avoid wasting polymer, the actual temperature was potentially slightly lower than the intended 170°C. This would mean that the crystalline phase would not have fully melted before pultrusion. Any crystals in the melt would give rise to nucleation sites on cooling and promote crystallization in the polymer. An incomplete melt would, however, be anticipated to suppress shear-induced crystallization in the pull direction. If this theory is correct, the 190°C samples, after having reached the fully amorphous state, would undergo more orderly recrystallization in the direction of pulling, strengthening the tapes to a larger extent and perhaps being responsible for the higher strength and stiffness of the 190°C samples.

This conjecture can be verified by further analysis such as direct measurement of the samples' degree of crystallinity and more exact monitoring of the melt pool temperature. Furthermore, the analysis of the failure mode of the tapes would also be beneficial for determining the reasons the tapes always fail outside the weld surface. While the failures near the clamps could be attributed to the stress concentrations that arise from improper clamping, the welded section appears to be stronger than the non-welded sections because just one specimen broke in the welded section. This needs to be examined more closely, e.g., through cross-sectional analysis of the welded area, to improve the knowledge of the interface between the two tapes to be welded. Furthermore, examination of the crystallinity of the weld zone, which was likely altered by the "reprocessing" of the thermoplastic during the welding operation, can lead to an understanding of the mechanical performance of the weld.

Finally, when comparing the pultruded tapes with the benchmark tapes, there was a significant difference in mechanical properties. Both the 170°C and 190°C samples performed much better, due to the loosely bound nature of the fibres in the benchmark samples. MicroCT imaging of the benchmark tapes reveals minimal thermoplastic matrix surrounding the fibres (Figure 53), which will hinder effective stress transfer in the composite and cause it to tear more easily. In addition, the lack of a thermoplastic-rich layer on the surface of the benchmark tapes makes it challenging to achieve a good weld.

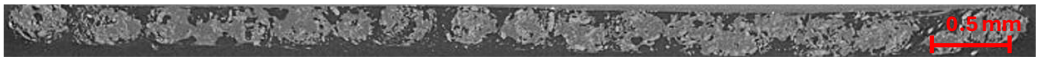

Figure 53: MicroCT of the BPREG 50vf% benchmark sample

5. Conclusion

In this study, the full assessment of pultrusion processing of flax/PP composite tapes was conducted in pursuit of an optimization of the processing parameters to enhance the quality of the tapes. The entire work was divided into two phases of testing that provided useful information regarding the effects of temperature, pulling speed, die design, and number of fibre yarns on the properties of flax composite tapes.

To begin with, special attention was paid on surface texture and fibre impregnation at various conditions in the first testing stage. Rougher surface texture was normally found on samples produced at elevated melt pool temperatures (180/190°C) and higher pulling speed, mainly as a result of sloughing phenomena. The result of this phenomenon was quite evident at 190°C and 90mm/min, due to the polymer/metal adhesion surpassing the strength of the pultrudate, leading to the fragments sticking on the die and tearing off the surface, thus worsening the surface quality. Additionally, the die geometry with short straight section was identified to be suboptimal because residence time of tapes in this type of die is too brief for it to become well-consolidated before leaving the die. Such lack of consolidation likely caused the yarns to relax and protrude out of the matrix, also contributing to surface roughness. By analysing the tapes produced at 160°C it was found that they were the least impregnated ones, and they showcased the highest surface roughness across all the samples, both of which are most probably related to the high viscosity of the polymer at that temperature.

From the first testing stage, it was revealed that using only 27 yarns heavily limits the testing, especially at high temperatures. When using 27 yarns, large fibre gaps were observed between the yarns, this made it challenging for the polymer matrix to completely fill them, leading to an increase in surface roughness as seen in the 180/190°C samples. To address this problem, the fibre count was increased in order to decrease fibre spacing and hence surface irregularities. In general, this first phase provided background information, which revealed that the short straight die arrangement and low yarn count were not ideal to make smooth, well-consolidated tapes.

Based on these results, a second testing phase was carried out with several efforts to enhance tape quality, particularly surface texture and mechanical properties. The yarn count was increased to 30, which seemed to have a noticeable effect on the surface texture by reducing gaps between fibres and allowing more effective matrix impregnation. This introduced an improvement, resulting in a more levelled surface in the 190°C specimens, where further yarns seemed to counteract some of the voids and gaps which afflicted the first testing phase samples. The long straight die configuration remained of much interest due to the superior performance during the first phase because of its longer residence time. On the other hand, the effect of changing the length of the tapered die could not be properly studied due to some design issues. Consequently, differences between the two configurations in the case of a short and long taper observed in the present study must be reassessed.

These findings indicated that, in addition to the surface texture enhancements observed, increased temperature processing can provide a range of other benefits. In fact, samples

processed at 190°C exhibited improved lap shear strength and stiffness than those processed at 170°C. This improvement in mechanical properties is probably a result of differences in degree of crystallization in the tapes, however, additional testing is required in order to fully understand how such temperatures affect crystallization.

The present work has contributed significantly to the optimization of flax/polypropylene composite tape pultrusion parameters, and it has been confirmed that all the investigated factors (die configuration, pulling speed, temperature, and yarn count) are involved in controlling the quality of the tape to various extents. The quality of pultruded natural fibre composites can be further improved by increasing the yarn count or modifying the die geometry. In addition, more accurate determinations of direct crystallinity and advanced cross-sectional analysis methods can be used to enhance the process. This study paves the way for the creation of still greener and more efficient composite production processes utilizing natural fibres as reinforcement in thermoplastic matrices to meet the industry's needs for greener materials.

6. Future Research Recommendations

To explore the findings of this study further and address some of the observed limitations, possible future research directions include modifications to: yarn count, die design, crystallization analysis, and void measurement techniques.

Yarn Count and Consolidation: While the addition of more than 27 yarns had positive effects on surface texture, it is possible in future studies to establish what numbers of yarns should be added to achieve optimal surface texture. This will help to identify a fibre density which will optimize mechanical properties without the addition of void content.

Maximize Die Design for Optimal Thickness Control: This present study had thicker tapes as a result of a die design flaw, and thus long-tapered die configurations had unclear impacts on the properties. Optimization of the die design would allow the evaluation of the true effect of taper length on consolidation, surface texture, and strength.

Detailed Crystallization Analysis: Since crystallization is known to influence mechanical properties of semi-crystalline thermoplastics, evaluating the degree of crystallinity at the different processing temperatures might be able to provide a better understanding of the lap-shear result, and allow for optimization of the manufacturing process.

Advanced Void Analysis Techniques: Owing to the challenges in void analysis, estimation might be better achieved by other imaging techniques. This would yield a better understanding of the role played by processing conditions on void content.

References

1. *Special Report 22/2023: Offshore Renewable Energy in the EU*.
2. Lichtenegger, G., Rentizelas, A. A. & Trivyza, N. Offshore and onshore wind turbine blade waste material forecast at a regional level in Europe until 2050. *Waste Management* **106**, 120–131 (2020).
3. Beauson, J., Laurent, A., Rudolph, D. P. & Pagh Jensen, J. The complex end-of-life of wind turbine blades: A review of the European context. *Renewable and Sustainable Energy Reviews* **155**, (2022).
4. Shuaib, N. A. & Mativenga, P. T. Energy demand in mechanical recycling of glass fibre reinforced thermoset plastic composite. *J Clean Prod* 198–206 (2016).
5. Song, Y. S., Youn, J. R. & Gutowski, T. G. Life cycle energy analysis of fiber-reinforced composites. . *Compos Part A Appl Sci Manuf* (2009).
6. Yu Fu, W. *Carbon Footprint and Sustainability of Different Natural Fibres for Biocomposites and Insulation Material*. www.nova-institut.eu (2019).
7. Pil, L., Bensadoun, F., Pariset, J. & Verpoest, I. Why are designers fascinated by flax and hemp fibre composites? *Compos Part A Appl Sci Manuf* **83**, 193–205 (2016).
8. Rybicka, J., Tiwari, A., Alvarez Del Campo, P. & Howarth, J. Capturing composites manufacturing waste flows through process mapping. *J Clean Prod* (2015).
9. Vedernikov, A., Safonov, A., Tucci, F., Carlone, P. & Akhatov, I. Pultruded materials and structures: A review. *Journal of Composite Materials* vol. 54 4081–4117 Preprint at https://doi.org/10.1177/0021998320922894 (2020).
10. Minchenkov, K., Vedernikov, A., Safonov, A. & Akhatov, I. Thermoplastic Pultrusion: A Review. (2021) doi:10.3390/polym.
11. Pil, L., Bensadoun, F., Pariset, J. & Verpoest, I. Why are designers fascinated by flax and hemp fibre composites? *Compos Part A Appl Sci Manuf* **83**, 193–205 (2016).
12. Van De Velde, K. & Kiekens, P. Thermoplastic pultrusion of natural fibre reinforced composites. *Compos Struct* **54**, 355–360 (2001).
13. Elfaleh, I. *et al.* A comprehensive review of natural fibers and their composites: An eco-friendly alternative to conventional materials. *Results in Engineering* vol. 19 Preprint at https://doi.org/10.1016/j.rineng.2023.101271 (2023).
14. Elfaleh, I. *et al.* A comprehensive review of natural fibers and their composites: An eco-friendly alternative to conventional materials. *Results in Engineering* vol. 19 Preprint at https://doi.org/10.1016/j.rineng.2023.101271 (2023).
15. AL-Oqla, F. M. & Salit, M. S. Natural fiber composites. in *Materials Selection for Natural Fiber Composites* 23–48 (Elsevier, 2017). doi:10.1016/B978-0-08-100958-1.00002-5.
16. Malkapuram, R., Kumar, V. & Singh Negi, Y. Recent development in natural fiber reinforced polypropylene composites. *Journal of Reinforced Plastics and Composites* **28**, 1169–1189 (2009).

17. John, M. J. & Thomas, S. Biofibres and biocomposites. *Carbohydrate Polymers* vol. 71 343–364 Preprint at https://doi.org/10.1016/j.carbpol.2007.05.040 (2008).

18. Yan, L., Chouw, N. & Jayaraman, K. Flax fibre and its composites - A review. *Compos B Eng* **56**, 296–317 (2014).

19. Charlet, K., Eve, S., Jernot, J. P., Gomina, M. & Breard, J. Tensile deformation of a flax fiber. *Procedia Eng* **1**, 233–236 (2009).

20. Baley, C. Analysis of the flax fibres tensile behaviour and analysis of the tensile stiffness increase. *Compos Part A Appl Sci Manuf* **33**, 939–948 (2002).

21. Charlet, K. *et al.* Characteristics of Hermès flax fibres as a function of their location in the stem and properties of the derived unidirectional composites. *Compos Part A Appl Sci Manuf* **38**, 1912–1921 (2007).

22. Rahman, M. Z. Mechanical and damping performances of flax fibre composites – A review. *Composites Part C: Open Access* vol. 4 Preprint at https://doi.org/10.1016/j.jcomc.2020.100081 (2021).

23. Bos, H. L., Van Den Oever, M. J. A. & Peters, O. C. J. J. *Tensile and Compressive Properties of Flax Fibres for Natural Fibre Reinforced Composites*.

24. Pinto, D. G., Rodrigues, J. & Bernardo, L. A review on thermoplastic or thermosetting polymeric matrices used in polymeric composites manufactured with banana fibers from the pseudostem. *Applied Sciences (Switzerland)* vol. 10 Preprint at https://doi.org/10.3390/app10093023 (2020).

25. Katsiropoulos, C. V., Pantelakis, S. G., Barile, M. & Lecce, L. Development of a novel hybrid thermoplastic material and holistic assessment of its application potential. *Aerospace* **8**, (2021).

26. Review of Thermoplastic Composites in Aerospace Industry. *International Journal on Engineering Technologies and Informatics* **3**, (2022).

27. Vaidya, U. K. & Chawla, K. K. Processing of fibre reinforced thermoplastic composites. *International Materials Reviews* vol. 53 185–218 Preprint at https://doi.org/10.1179/174328008X325223 (2008).

28. Woigk, W. *et al.* Interface properties and their effect on the mechanical performance of flax fibre thermoplastic composites. *Compos Part A Appl Sci Manuf* **122**, 8–17 (2019).

29. Kickelbick, Guido. *Hybrid Materials : Synthesis, Characterization, and Applications*. (Wiley - VCH, 2007).

30. Gholampour, A. & Ozbakkaloglu, T. A review of natural fiber composites: properties, modification and processing techniques, characterization, applications. *Journal of Materials Science* vol. 55 829–892 Preprint at https://doi.org/10.1007/s10853-019-03990-y (2020).

31. Oliver Patrick Lythe McGregor. Manufacture and Characterisation of Natural Fibre Thermoplastic Composite Tapes. (University of Auckland, 2014).

32. R. Schledjewski & A. K. Schlarb. In-situ consolidation of thermoplastic tape material effects of tape quality on resulting part properties. *International SAMPE Symposium and Exhibition (Proceedings),* vol. 52 Preprint at (2007).

33. A. M. Vodermayer, J. C. Kaerger & G. Hinrichsen. Manufacture of high performance fibre-reinforced thermoplastics by aqueous powder impregnation. *Composites Manufacturing* (1993).

34. S. R. Iyer & L. T. Drzal. Manufacture of Powder-Impregnated Thermoplastic Composites. *Journal of Thermoplastic Composite Materials* (1990).

35. Risteska, S. *Unidirectional Carbon Fiber Reinforced Thermoplastic Tape in Automated Tape Placement Process*. www.intechopen.com.

36. Wiedmer, S. & Manolesos, M. An experimental study of the pultrusion of carbon fiber-polyamide 12 yarn. *Journal of Thermoplastic Composite Materials* **19**, 97–112 (2006).

37. G. M. Wu & J. M. Schultz. Processing and properties of solution impregnated carbon fiber reinforced polyethersulfone composites. *Polym Compos* (2000).

38. H. Bijsterbosch. Impregnation of glass rovings with a polyamide melt. *Composites Manufacturing* (1993).

39. S. R. Iyer & L. T. Drzal. Manufacture of Powder-Impregnated Thermoplastic Composites. *Journal of Thermoplastic Composite Materials* (1990).

40. McGregor, O. P. L., Somashekar, A. A., Bhattacharyya, D., McGregor, O. P. L. & Duhovic, M. Pre-impregnated natural fibre-thermoplastic composite tape manufacture using a novel process. *Compos Part A Appl Sci Manuf* **101**, 59–71 (2017).

41. Hartung, D. *et al.* Manufacturing and Analysis of Natural Fiber-Reinforced Thermoplastic Tapes Using a Novel Process Assembly. *Sustainability (Switzerland)* **15**, (2023).

42. Akonda, M. H., Shah, D. U. & Gong, R. H. Natural fibre thermoplastic tapes to enhance reinforcing effects in composite structures. *Compos Part A Appl Sci Manuf* **131**, (2020).

43. Kucher, M., Dannemann, M., Heide, A., Winkler, A. & Modler, N. Miniaturised rod-shaped polymer structures with wire or fibre reinforcement—manufacturing and testing. *Journal of Composites Science* **4**, (2020).

44. Alsinani N, G. M. L. L. L. Effect of cooling temperature on deconsolidation and pulling forces in a thermoplastic pultrusion process. (2021).

45. Alsinani, N. & Laberge Lebel, L. Effect of high pulling speeds on the morphologies of pultrudates in a thermoplastic pultrusion process. *Journal of Thermoplastic Composite Materials* **36**, 3566–3584 (2023).

46. Brennan, M. G. CFD Modeling of the Closed Injection Wet-Out Process For Pultrusion. (2008).

47. Tucci, F., Rubino, F., Pasquino, G. & Carlone, P. Thermoplastic Pultrusion Process of Polypropylene/Glass Tapes. *Polymers (Basel)* **15**, (2023).

48. G. L. Batch, C. W. M. Analysis of pressure, pulling force, and sloughing in pultrusion. *American Society of Mechanical Engineers, Heat Transfer Division, (Publication) HTD* (1990).

49. Ghaedsharaf, M. *et al*. *Thermoplastic Composite Rod Manufacturing Using Biaxial Braid-Trusion BIAXIAL BRAID-TRUSION*. http://www.polymtl.ca/labsfca/en (2018).

50. Alsinani, N., Ghaedsharaf, M. & Laberge Lebel, L. Effect of cooling temperature on deconsolidation and pulling forces in a thermoplastic pultrusion process. *Compos B Eng* **219**, (2021).

51. Ferreira, F., Fernandes, P., Correia, N. & Marques, A. T. Development of a pultrusion die for the production of thermoplastic composite filaments to be used in additive manufacture. *Journal of Composites Science* **5**, (2021).

52. D. Sharma & T. A. McCarty. Pultrusion die pressure response to changes in die inlet geometry. (2004).

53. Astrom, B. T., Larsson, H. & Byron, R. *Development of a Facility for Pultrusion of Thermoplastic-Matrix Composites*.

54. Hu, Y. *et al*. Influence of Cooling Rate on Crystallization Behavior of Semi-Crystalline Polypropylene: Experiments and Mathematical Modeling. *Polymers (Basel)* **14**, (2022).

55. Moitzi, J. & Skalicky, P. *Shear-Induced Crystallization of Isotactic Polypropylene Melts: Isothermal WAXS Experiments with Synchrotron Radiation*. (1993).